The infrared solar spectrum: diagnostics and methods

Tom Schad
National Solar Observatory / DKIST
2024 BBSO Summer School
1 August 2024



List of Useful References

1. Penn, M.J. Infrared Solar Physics. *Living Rev. in Solar Phys.*. *11*, (2014), 2
2. Harvey, J. and Hall. D., Magnetic Fields Measured with the 10830 ˚A He i Line", in Solar Magnetic Fields, Proceedings of IAU Symposium 43 held in Paris, France, August 31 – September 4, 1970, (Ed.) Howard, R., IAU Symposia, 43, p. 279, Reidel, Dordrecht.
3. Infrared solar physics: proceedings of the 154th Symposium of the International Astronomical Union; held in Tucson; Arizona; U.S.A.; March 2-6; 1992. D. M. Rabin, John T. Jefferies, and C. Lindsey. International Astronomical Union. Symposium no. 154; Kluwer Academic Publishers; Dordrecht
4. J. Heidt, Astronomy in the Near-Infrared - Observing Strategies and Data Reduction Techniques, Astrophysics and Space Science Library 467, https://doi.org/10.1007/978-3-030-98441-0_1
5. A. Rogalski, A. History of Infrared Detectors. *Opto-Electronics Review*. **20**(3), (2012) 279-308.
6. Stix. M. The Sun: An Introduction. 2nd Edition, Springer (2002).
7. Gray, D.F. The Observation and Analyis of Stellar Photospheres. Cambridge UP (2005).
8. Beletic, J.W. et al. Teledyne Imaging Sensors: Infrared imaging technologies for Astronomy & Civil Space. SPIE (2008)
9. Teague, J., Schmieder, D. The History of Forward-Looking Infrared (FLIR). DSIAC Publications DSIAC-2021-1342.

Lecture Outline

- **Defining the Infrared: A short history**
- The Infrared Solar Spectrum
  - Continuum formation and flare emission
  - Atomic lines of the lower atmosphere
  - Molecular species
  - Coronal emission
- Observing at Infrared Wavelengths
  - Advantages and disadvantages
  - Detectors
  - Optics
  - Cryostats
  - Coronagraphs
- Summary and Outlook
  - This afternoon's tutorial: Coronal IR Spectroscopy using DKIST/CryoNIRSP

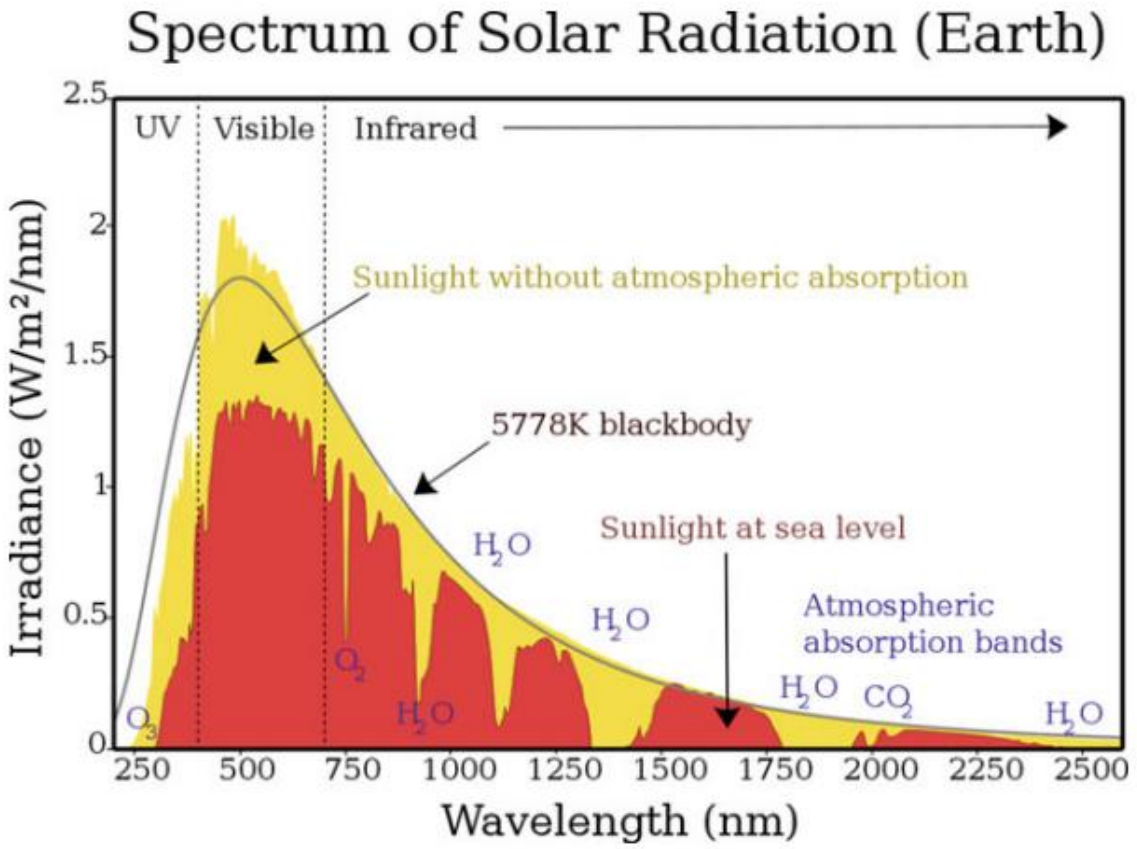

Defining “Infrared” – ‘infra’ is Latin for ‘below’

From the perspective of human vision, ‘infrared’ often refers merely to wavelengths longer than visible red (or ~> 650 nm). This motivates figures like those at left showing infrared starting around ~650 nm.

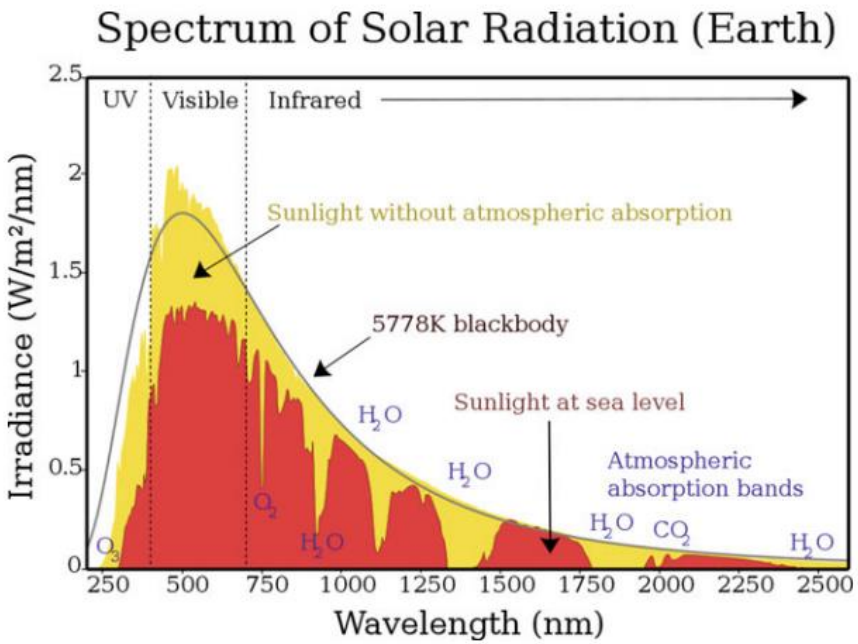

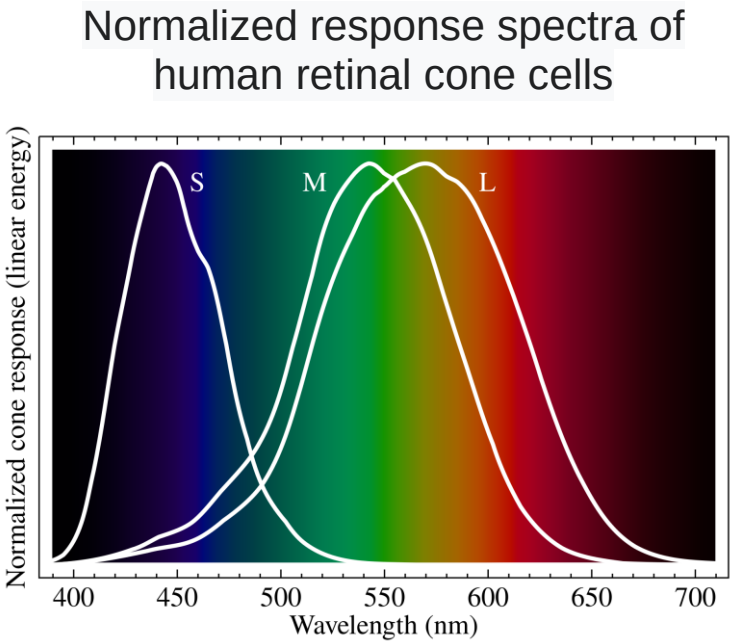

Yet, its important to understand that “infrared” is application specific. For example, in commercial domain, “IR photography” often refers to ~650 nm to ~900 nm whereas “IR imaging” often refers to thermal temperature mapping (or similar).

Defining “Infrared” and “Radiant Heat”

The History of Infrared Astronomy is directly tied to our ability to measure ‘invisible light’ from the ground.

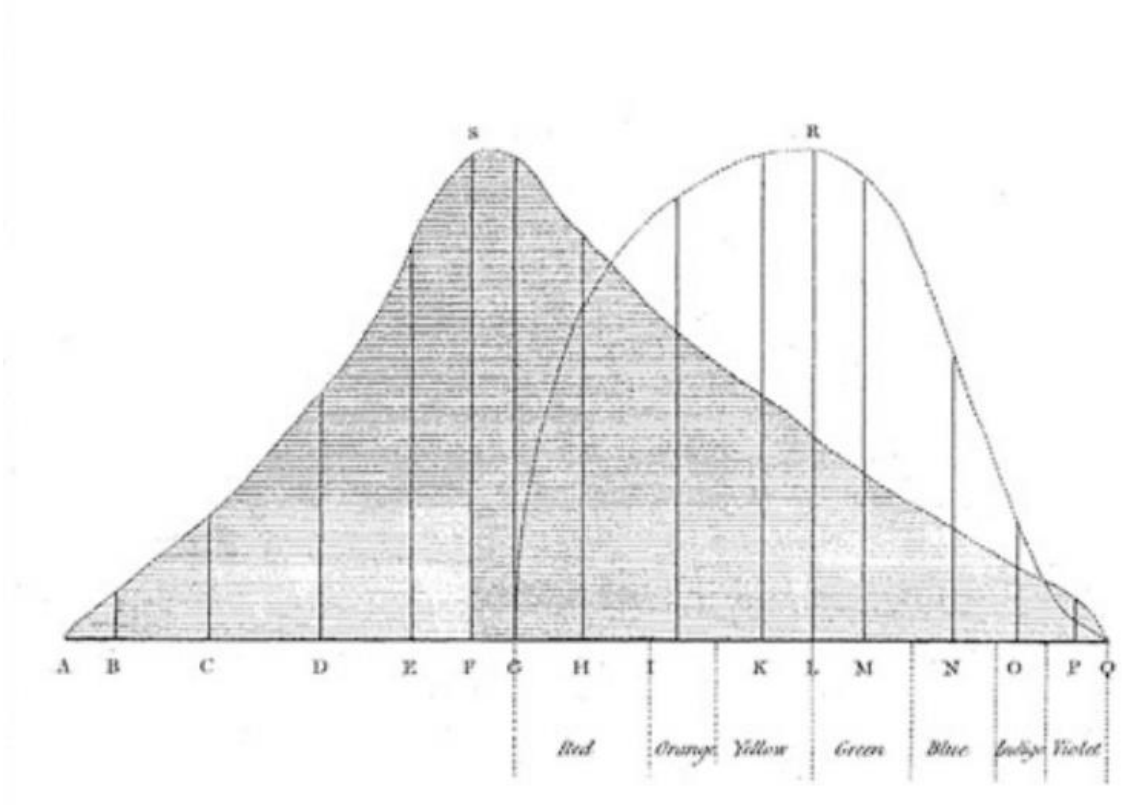

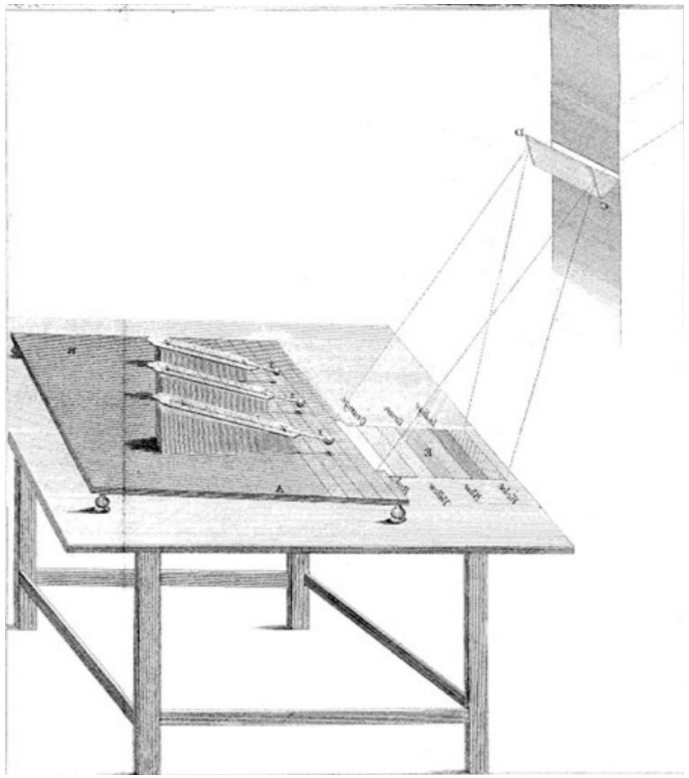

William Herschel (1800): visible and ‘radiant heat’ experiment with blackened thermometers to measure spectral energy distribution of the Sun. Reproduced from J. Heidt, *Astronomy in the Near-Infrared* (2022).

Fizeau and Foucault (1847): Improved observing methods show IR absorption bands on an early wavelength scale.

In 1845 they achieved first photographs of Sun in visible.

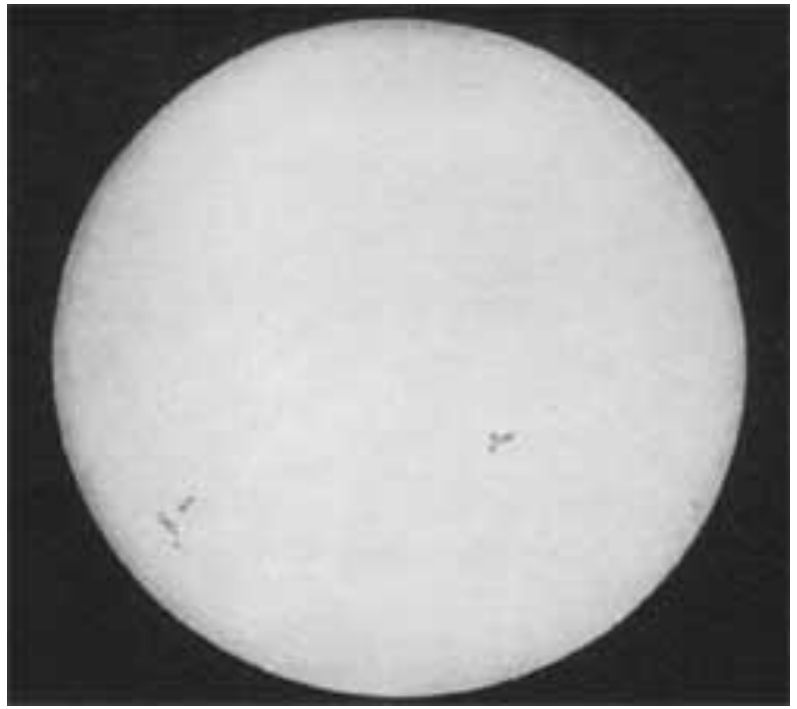

Measured with enclosed thermometer:
Reproduced from Lequeux (2009).

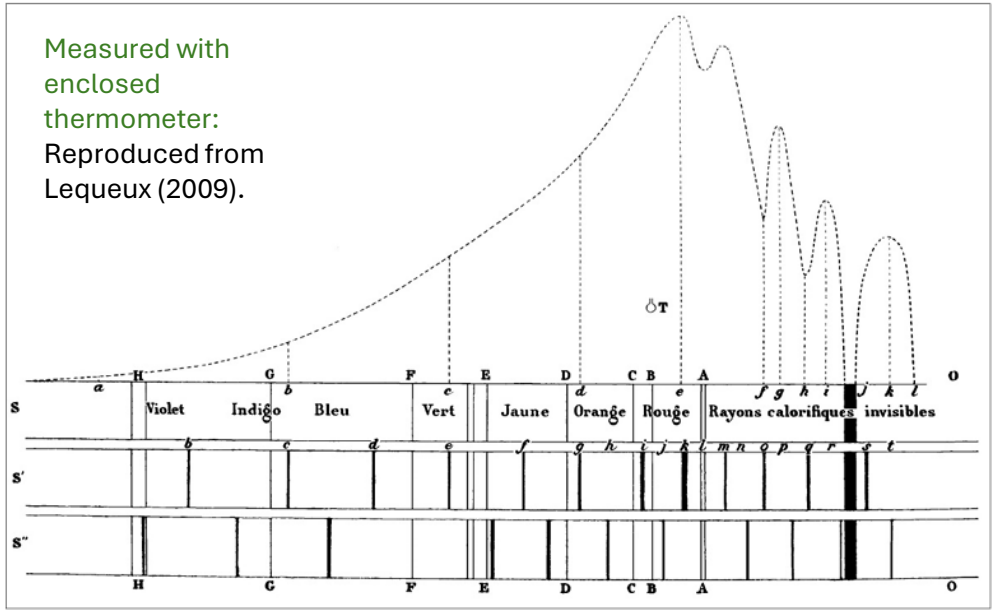

Figure 4: The spectrum of the Sun from the violet to the near infrared obtained by Fizeau and Foucault in 1847 with a glass prism. As for Figure 3, the spectrum, which would be expected to peak in the yellow, is in fact strongly displaced towards the infrared due to the variation of dispersion of the prism with wavelength. Fizeau and Foucault observed the infrared absorption bands due to the Earth's atmosphere, but they were not recognized as such by them. The vertical lines in S are the main Fraunhofer lines. The broad infrared bands were already suspected in 1843 by John William Draper (1811–1882) and also by John Herschel, but with no wavelength measurements.[3] In S′ and S″, the bold vertical lines mark the positions of interference fringes obtained using chromatic polarization, which are equidistant in wavelength. For the first time, they allowed the establishment of a wavelength scale in the near infrared.

1845: Kirchhoff and Bunson identified Fraunhofer lines as correlated to heated elemental emission. They also noted O2 molecular absorption features.

J.W. Draper discussed infrared bands around 1847 as well, founding later work by Angstrom and others.

Recall that Max Planck introduced blackbody law in 1901.

Langley (1888) using his invented bolometer device and a rock salt prism measured solar spectrum out to ~5 μm

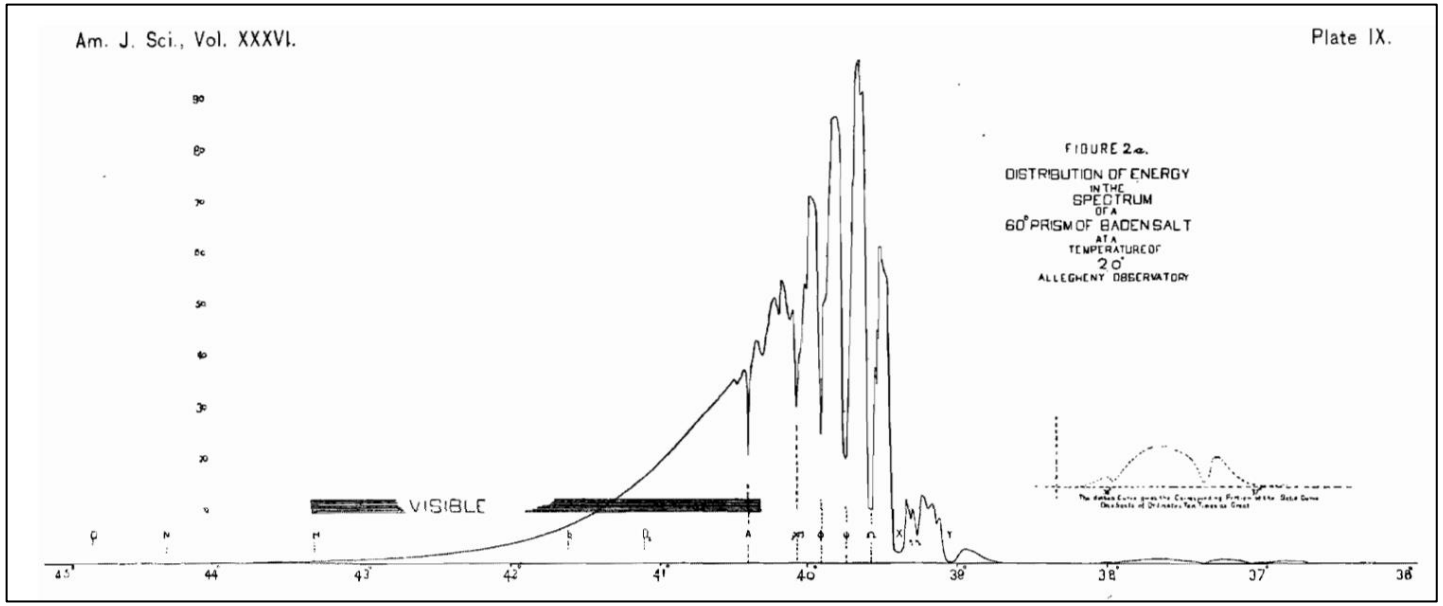

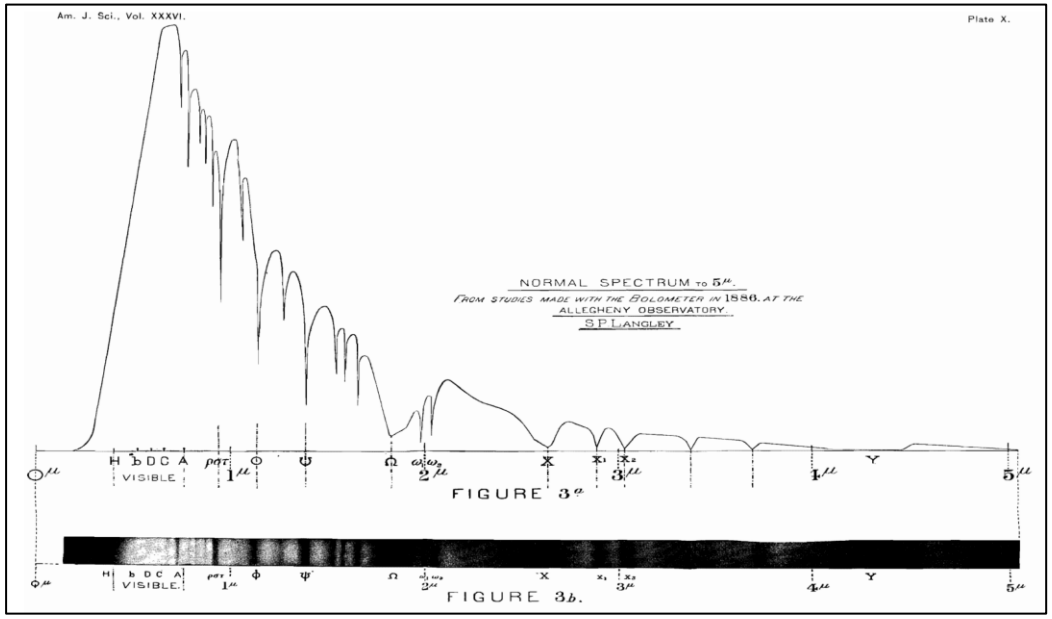

While bolometers were a major breakthrough (still in use) they did not provide the sensitivity, nor imaging capabilities of **early film based visible astronomy**.

IR astronomy research was not largely adopted until the development of new IR sensing technologies based on semiconductors (select milestones below, see e.g. Rogalski 2012):

1904: J.C. Bose patented the first IR photovoltaic detector
1930: PbS quantum detectors used first by German military for heat-direction finding. 30 km detection of ships. (US had been focused on radar and IR cells for communication)
1940: WW2: US National Defense Research Committee (NRDC) formed.
1941: NRDC asked Northwestern Professor R.J. Cashman to investigate IR cells.
1946: PbS cell figures for wavelength sensitivity (etc.) declassified. 1000x increase!

Cashman PbS Cell

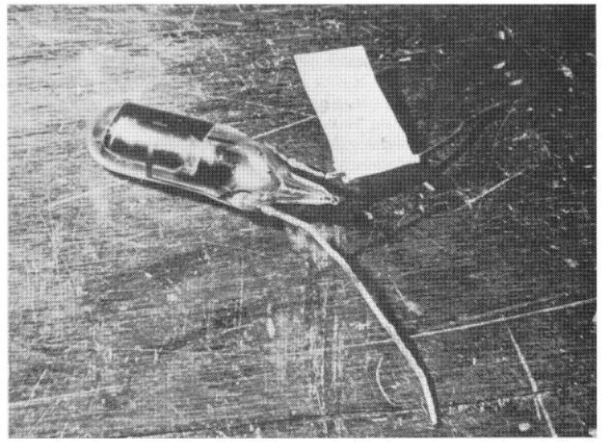

An early Cashman PbS cell, c. 1945. *(Photographed by the author at Cashman's Northwestern University Laboratory in Evanston, Illinois)*

1947: Kuiper, Wilson, and Cashman used PbS cell at McDonald Observatory to discover CO2 and CH4 bands of Mars and Titan.

1947: McMath, Mohler, Goldberg use Cashman PbS cells for infrared solar spectroscopy at McMath-Hulbert Observatory in Michigan, laying ground-work for IR solar physics later at McMath-Pierce Solar Telescope on Kitt Peak.

1961: U, B, V photometric system extended to include J, H, K bands centered within atmospheric transmission bands (Johnson 1961).

1970: CCDs invented; Silicon arrays for visible use expand fast; IR focal plane arrays (FPAs) follow suit.

What then is “Infrared” for Solar Physics and Astronomy?

The lower wavelength limit is typically defined as either:

1. The limit of human eye response: ~ 700 nm
2. The wavelength of the band gap for Silicon.
   -> Band gap is 1.14 eV or ~1090 nm.

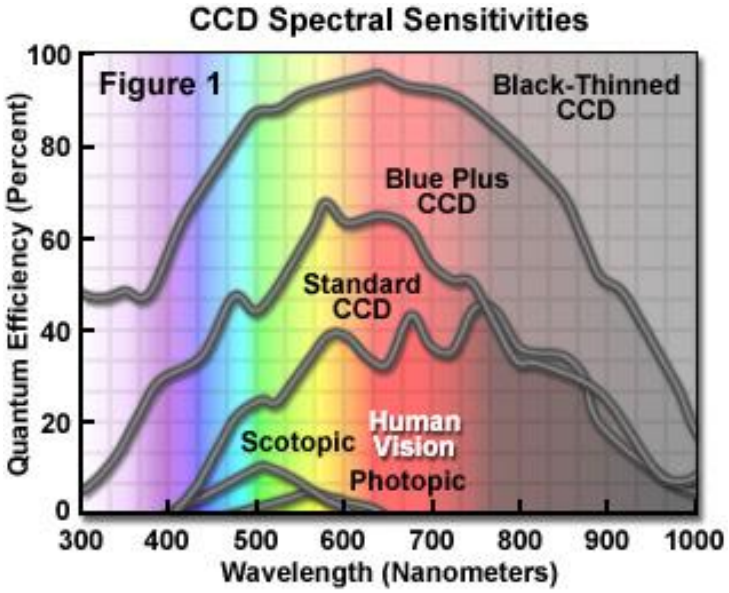

*Quirk: DKIST “**visible**” typically includes wavelengths to at least the Ca II “**infrared**” triplet near 850 nm.*

The upper wavelength limit is similarly fuzzy. Often cutoff is ~ 1mm (overlaps with sub-mm). ~25 μm is upper end of “Mid-IR” (defined by atmospheric windows).

Penn (2014) Living Review in Solar Physics notes the following IR regions:

Table 1: Informal Infrared Nomenclature.

Name	Wavelength [nm]	Wavenumber [cm^{-1}]	Frequency [GHz]	Temperature [K]
Near IR	700 – 5000	14 300 – 2000	428 000 – 60 000	4100 – 580
Mid-IR	5000 – 25 000	2000 – 400	60 000 – 12 000	580 – 120
Far-IR	25 000 – 10^6	400 – 10	12 000 – 300	120 – 3

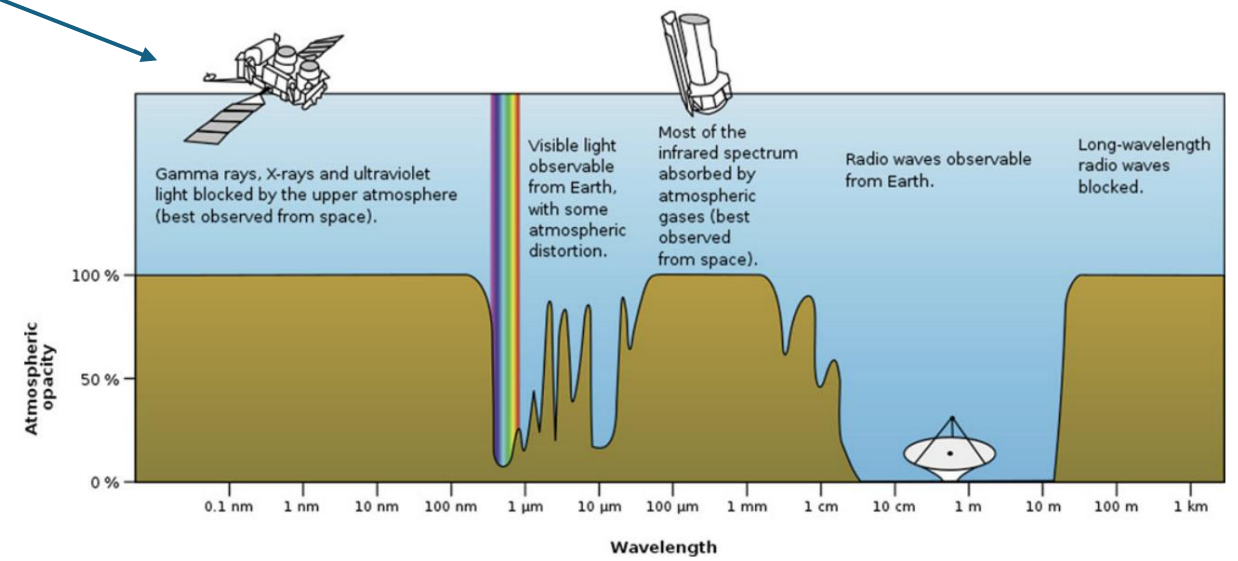

In this talk, we will mostly concentrate on 1 to ~10 μm.

Units and conversions in infrared astronomy

Wavelengths: 1000 nm = 10,000 Å = 1 μm (micrometer or 'micron')

(Temporal) Frequency = ν = c / λ Energy = hν = [4.1357e-15 eV s] * (c/λ)

Wavenumbers (spatial frequency) are often used especially due to Fourier Transform spectroscopy:

$$\tilde{\nu} = \frac{1}{\lambda}$$ *For units of cm^{-1}, $= 10^7$ / [wavelength in nm]*

Brightness temperature by Wien's law:

T ~ [2898 μm K] / λ

Table 1: Informal Infrared Nomenclature.

Name	Wavelength [nm]	Wavenumber [cm^{-1}]	Frequency [GHz]	Temperature [K]
Near IR	700 – 5000	14 300 – 2000	428 000 – 60 000	4100 – 580
Mid-IR	5000 – 25 000	2000 – 400	60 000 – 12 000	580 – 120
Far-IR	25 000 – 10^6	400 – 10	12 000 – 300	120 – 3

Vacuum to Air Wavelength Differences:

$\lambda_{air} = \lambda_{vac} / n_{air}$

$n_{air} = 1 + 0.0000834254 + 0.02406147 / (130 - s^2) + 0.00015998 / (38.9 - s^2)$,
where $s = 10^4 / \lambda_{vac}$ and λ_{vac} is in Å
Airtovac: see https://www.astro.uu.se/valdwiki/Air-to-vacuum%20conversion

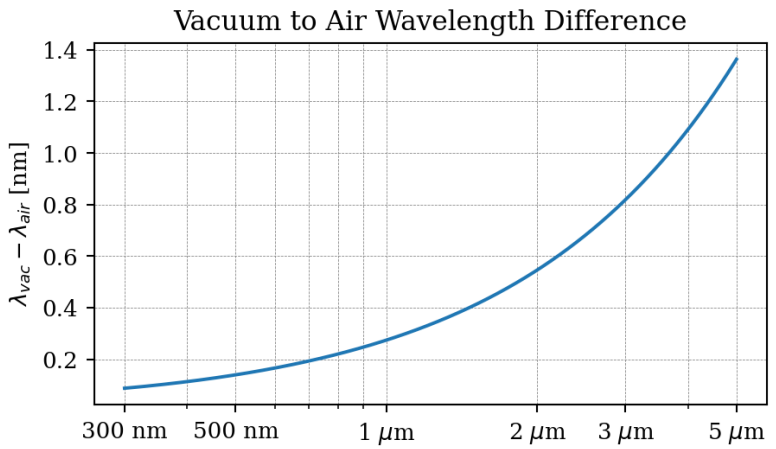

Lecture Outline

- Defining the Infrared: A short history
- **The Infrared Solar Spectrum**
  - Continuum formation and flare emission
  - Atomic lines of the lower atmosphere
  - Molecular species
  - Coronal emission
- Observing at Infrared Wavelengths
  - Advantages and disadvantages
  - Detectors
  - Optics
  - Cryostats
  - Coronagraphs
- Summary and Outlook
  - This afternoon's tutorial: Coronal IR Spectroscopy using DKIST/CryoNIRSP

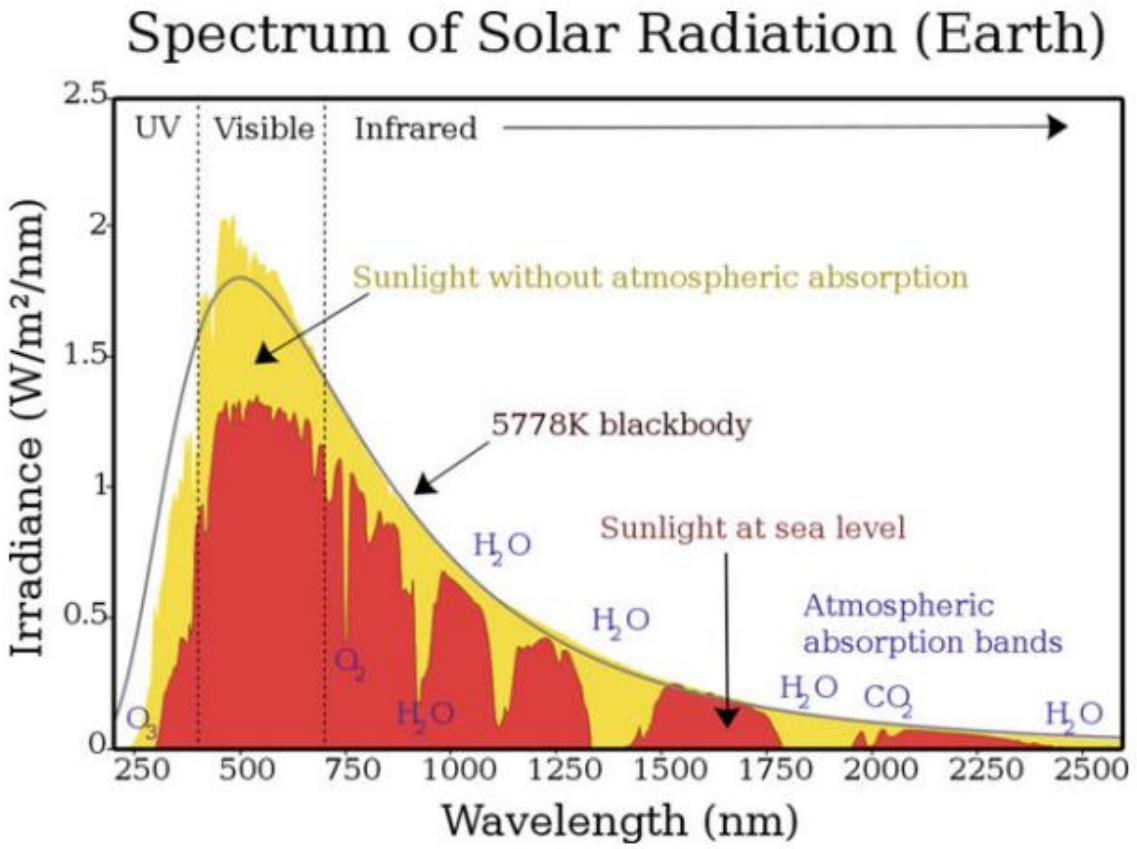

The Infrared Solar Continuum

At long wavelengths, Planck's law becomes the Rayleigh-Jeans law

$$B_\lambda(T) \approx \frac{2c}{\lambda^4} k_B T$$

However, the Sun's spectral distribution is not a perfect blackbody of a single temperature.

Transitioning from Visible to IR, the dominant continuum opacity sources switches from H-minus bound-free to H-minus free-free.

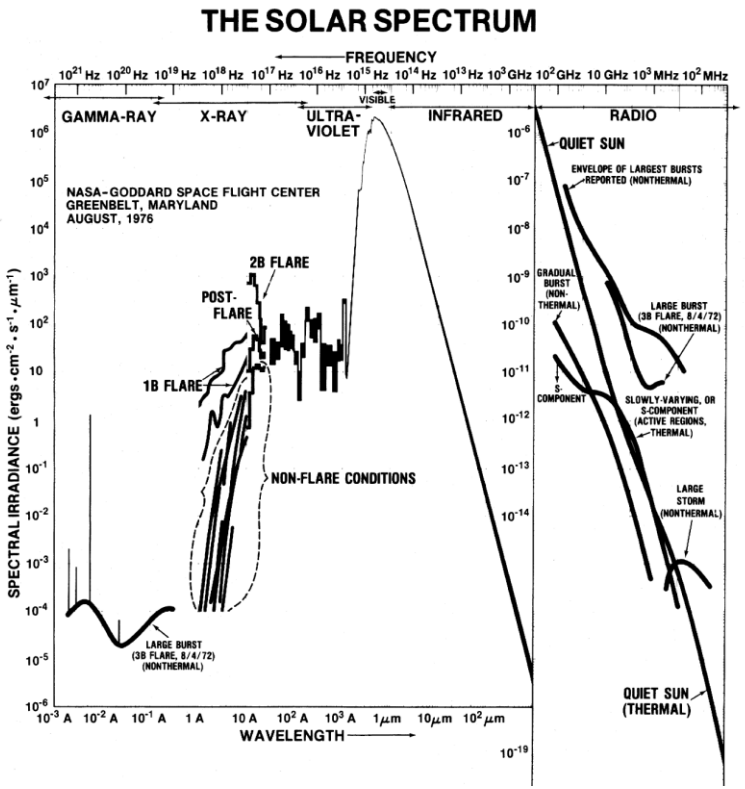

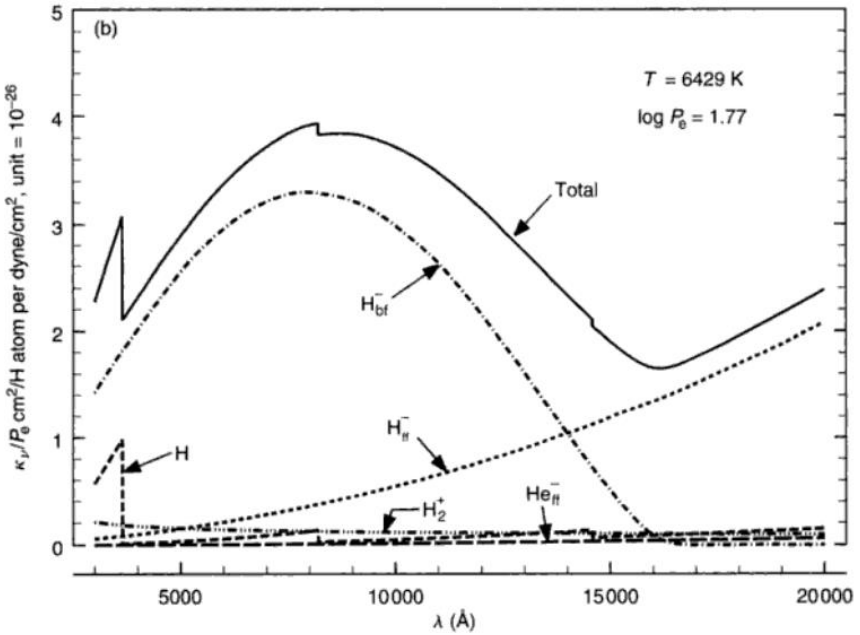

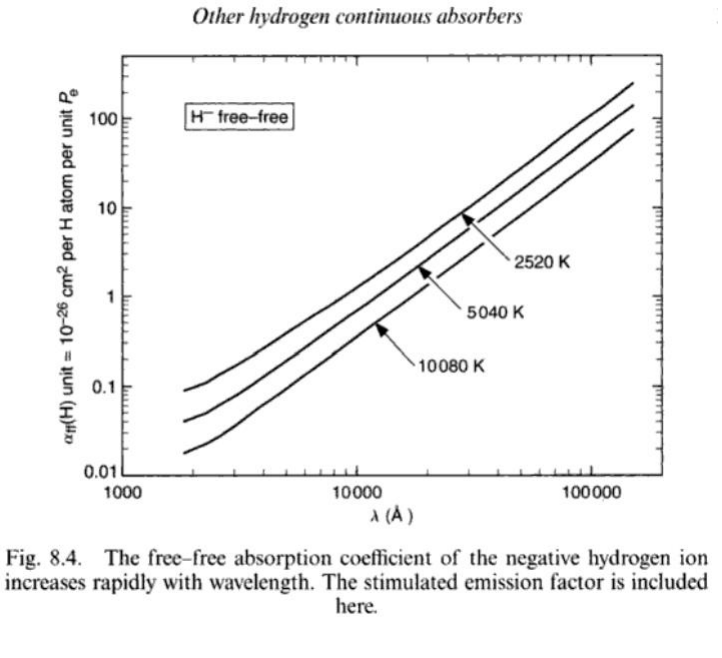

Fig. 8.4. The free–free absorption coefficient of the negative hydrogen ion increases rapidly with wavelength. The stimulated emission factor is included here.

Figure 8.4 and 8.5(b) from Grey, D.F. *Stellar Photospheres*

Consequences of the transition from H-bf to H- ff continuous opacity:

1. Near 1.6 micron, the photons come from the deepest optically accessible layer of the Sun. That is, it has the highest brightness temperature.
2. H- ff absorption increases with wavelength, meaning the continuum progressively samples the lower atmosphere.

Vernazza et al. (1976)

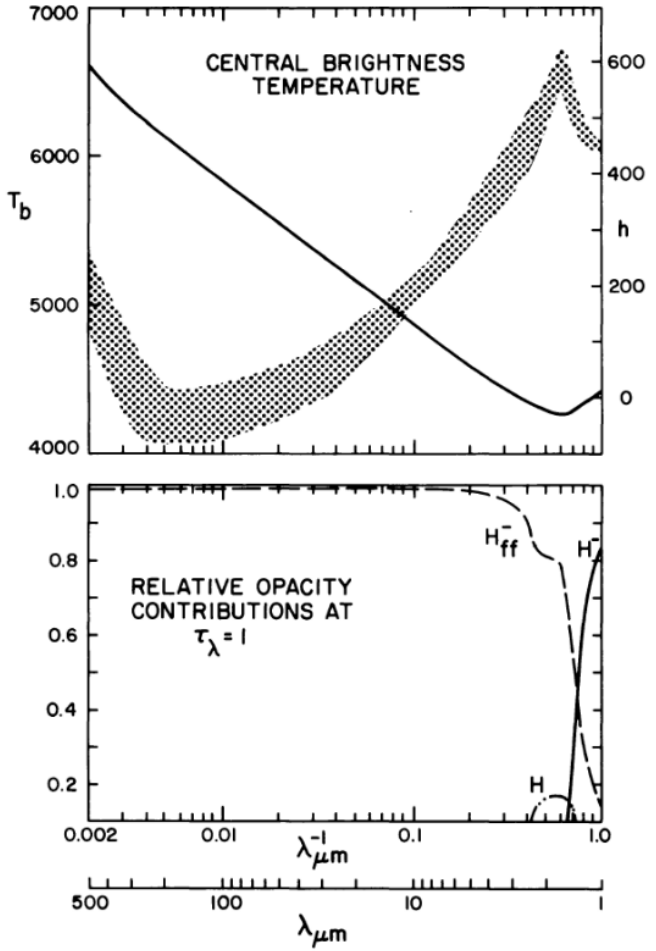

J.T. Jefferies (1994)

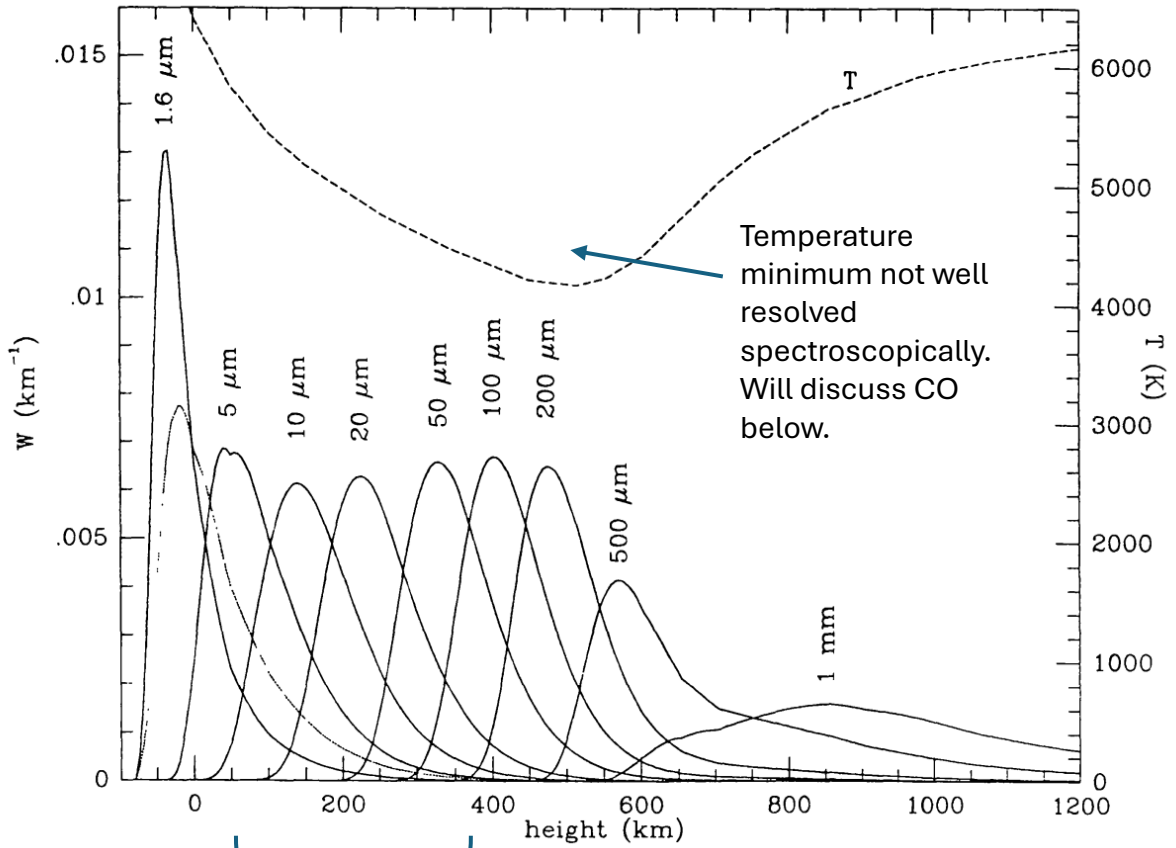

Temperature minimum not well resolved spectroscopically. Will discuss CO below.

Very few continuum measurements despite relative simplicity of interpretation.

ALMA

Continuum observations at long wavelengths:

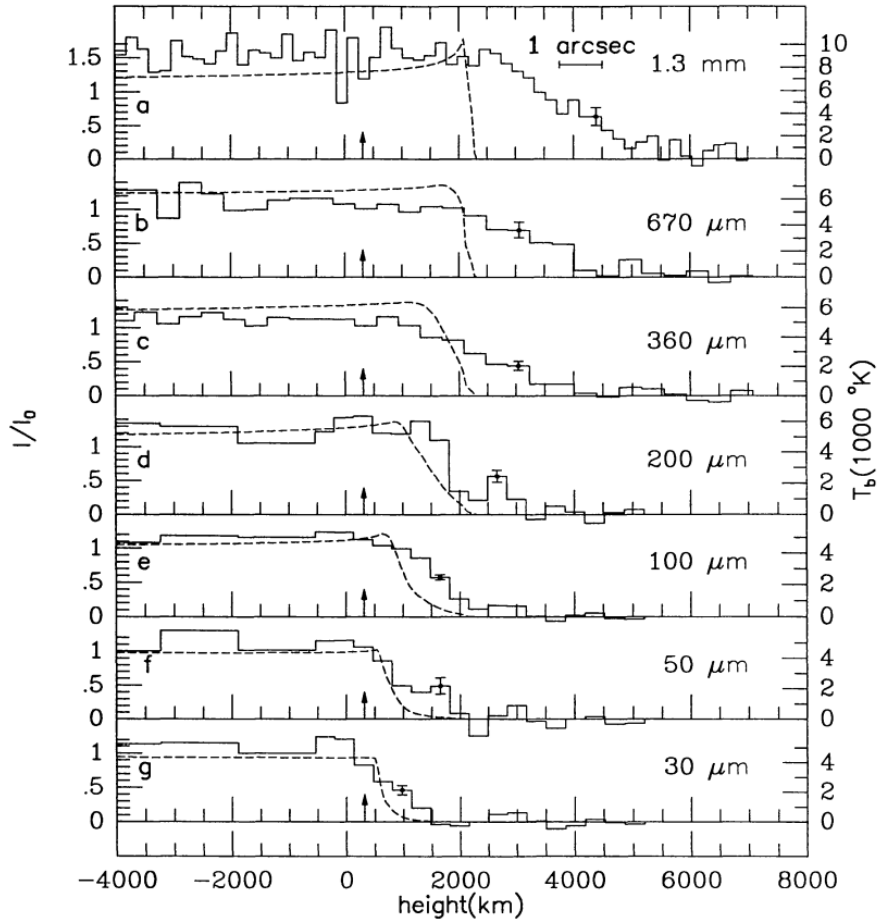

Fig. 4. Limb brightness profiles determined by occultation at total solar eclipses. Panel *a* is for 1991 July 11 (Lindsey *et al.* 1992,); *b* and *c* are for 1987 March 18 (Roellig *et al.* 1991); and *d*, *e*, *f*, and *g* were for the 1981 July 31 eclipse (Lindsey *et al.* 1986.)

James Clerk Maxwell Telescope (Hawaii)

Menezes et al. (2022)

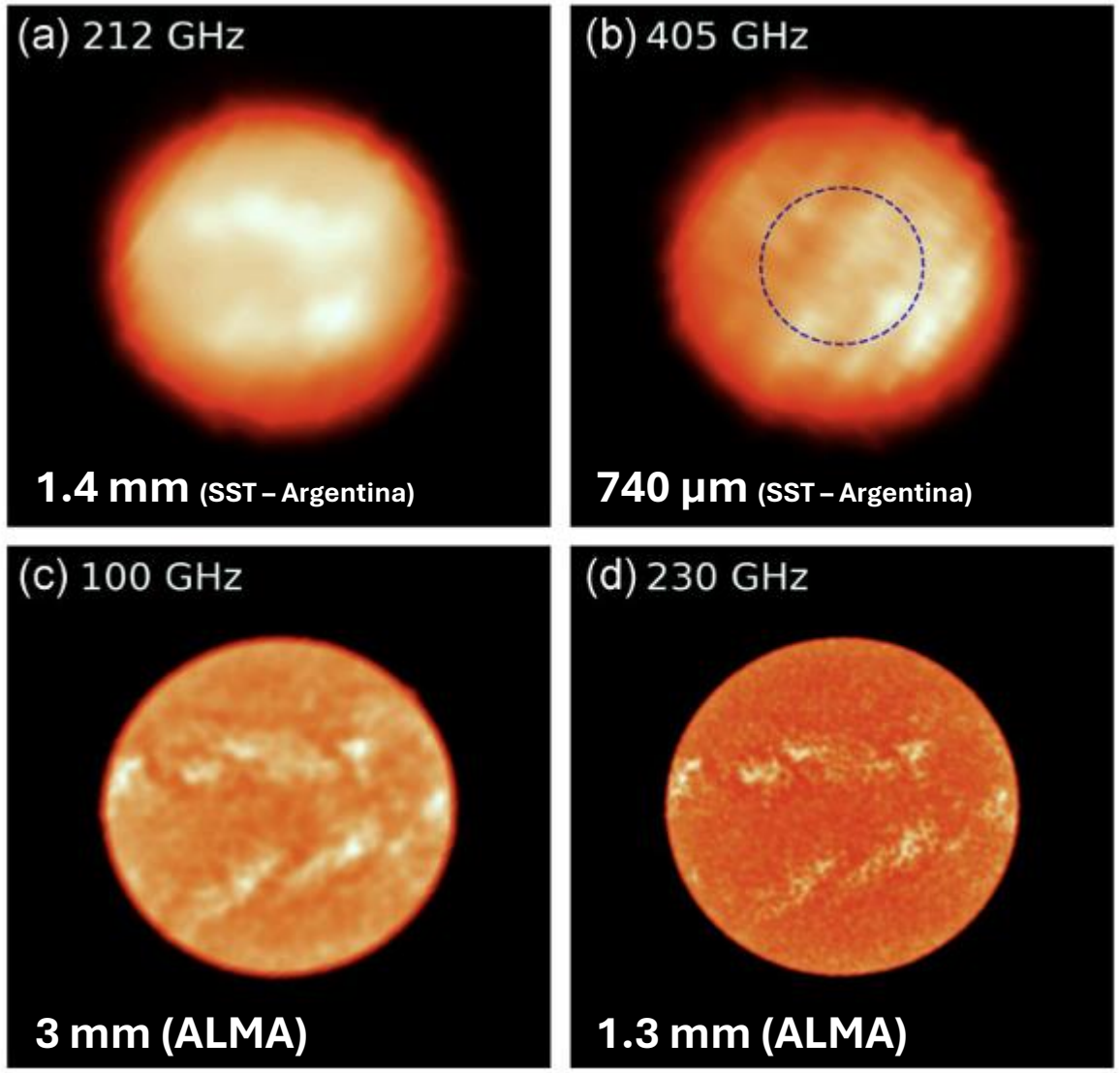

The Infrared Solar Continuum: Flare Emission

Penn et al. (2016)

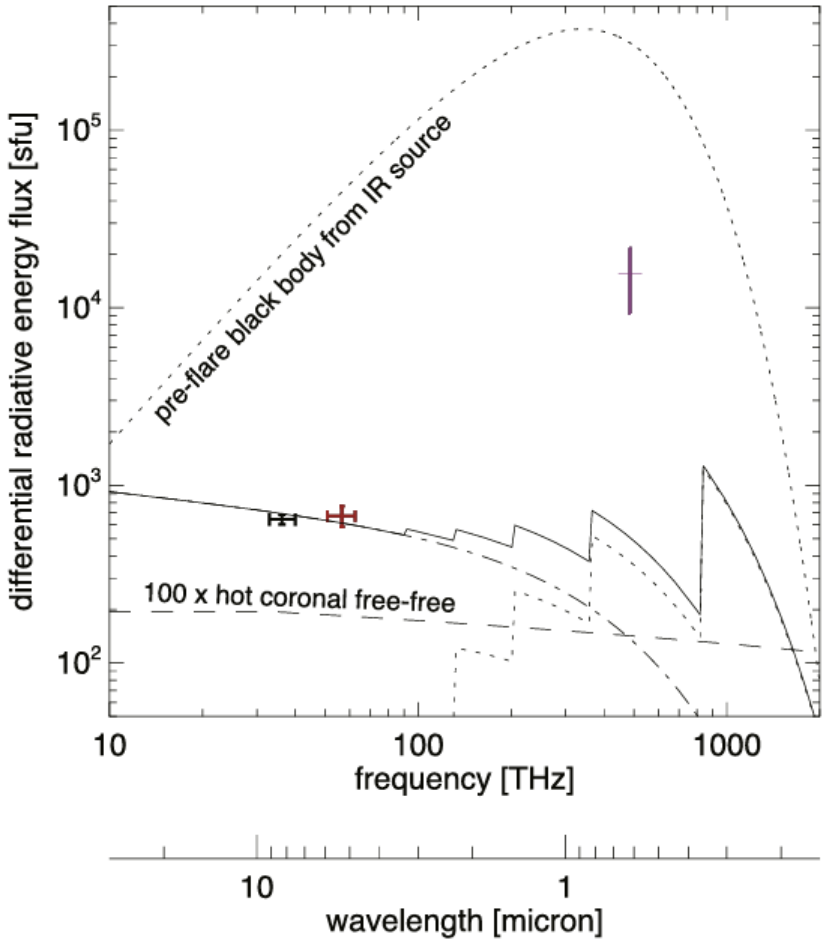

Simoes et al. (2017) argue IR continuum via ion free-free emission is direct indicator for atmospheric ionization during flares.

Using a QWIP dual-channel detector at the McMath-Pierce Solar Telescope

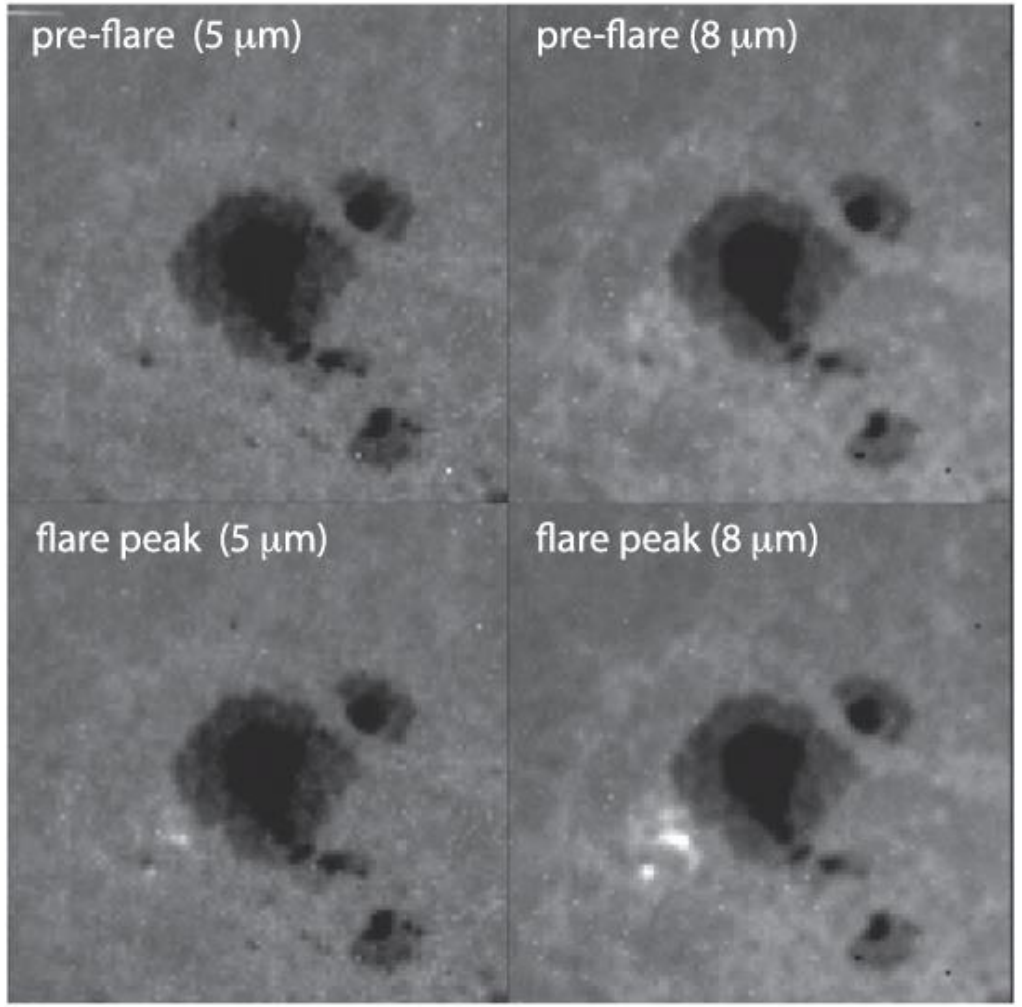

Figure 1. Snapshot raw images: pre-flare (top), flare peak (17:49:20 UT; bottom), with 5 μm (left) and 8 μm (right).

Atomic Lines in the Solar Atmosphere

The number of atomic spectral lines decreases in infrared as the energy difference implies lower populated upper energy states.

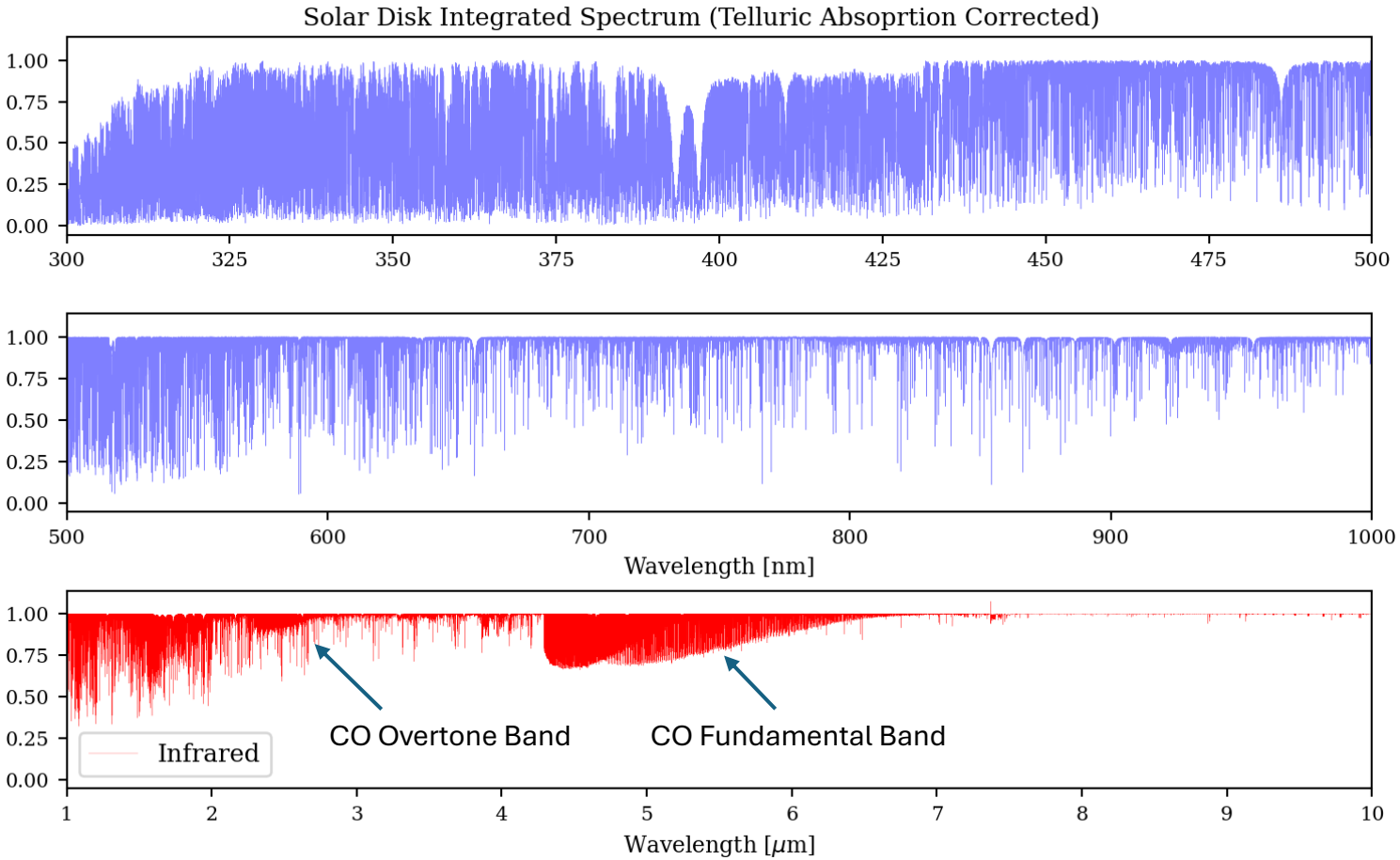

Infrared transition energies:

1.24 eV @ 1 micron

0.25 eV @ 5 micron

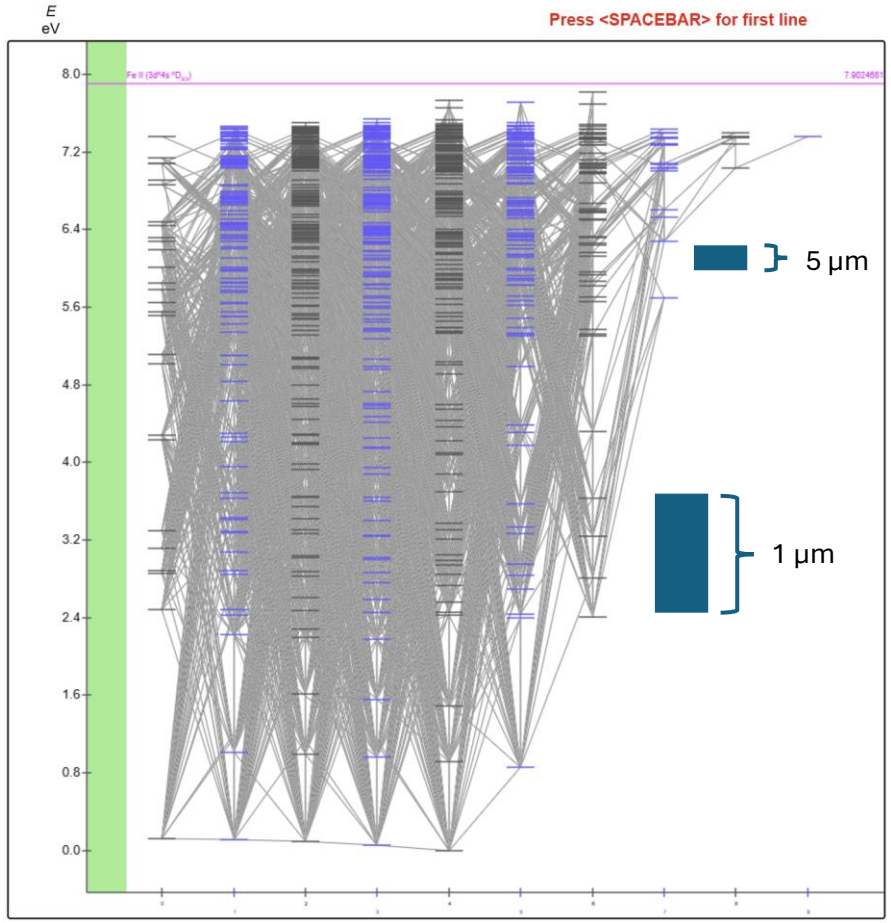

NIST Grotrian Diagram For Fe I

Eneregy Level [eV] by J state

Lower energy transitions does mean the infrared contains more rovibrational molecular transitions (both from the Sun and Earth's atmosphere!)

IR Atomic Lines: Increased Zeeman Sensitivity

The Doppler broadened width of LTE lines increase linearly with its wavelength

$$\Delta\lambda_{\rm D} = \frac{\lambda_0^2}{c}\,\Delta\nu_{\rm D} = \lambda_0\,\frac{w_{\rm T}}{c}$$

$$w_{\rm T} = \sqrt{\frac{2k_{\rm B}T}{\mu M} + \xi^2}$$

Meanwhile, the Zeeman Effect induced line splitting increases with $g_{eff}\lambda^2$

$$\lambda^{JJ'}_{MM'} = \lambda_0 - \Delta\lambda_B\,(g'M' - gM)$$

$$\Delta\lambda_B = \lambda_0^2\,\frac{\nu_{\rm L}}{c} = \frac{\lambda_0^2\,e_0\,B}{4\pi mc^2}$$

A relative "magnetic sensitivity" parameter can be defined as $g_{eff}\lambda$.

Intense field regime occurs when $\frac{\Delta\lambda_{\rm B}}{\Delta\lambda_D} \gg 1$.

Penn (2014)

Table 2: Magnetic Sensitivity of Spectral Lines

Region	Atom	Wavelength [nm]	$g_{\rm eff}$	$\lambda g_{\rm eff}$	
Photosphere	Fe I	525	3.0	1575	
	Fe I	630	2.5	1575	Opacity Minimum
	Fe I	1565	3.0	4695	
	Ti I	2231	2.5	5778	
	Fe I	4064	1.25	5080	
	Fe I	4137	2.81?	11625 ?	Very strong splitting
	Mg I	12318	1.0	12318	
Chromosphere	Ca I	854	1.1	939	
	Mg I	3682	1.17	4307	Unexplored
	Ca I	3697	1.1	4067	
Corona	[Fe XIV]	530	1.33	706	
	[Fe XIII]	1075	1.5	1612	Coronal B
	[Si X]	3934	1.5	5901	

In intense regime, field strength can be measured spectroscopy and is less susceptible to filling factor assumptions.

Equations from E. Landi Degl'Innocenti & M. Landolfi (2004)

IR Atomic Lines: Increased Zeeman Sensitivity

Qualitative visual of enhanced splitting at Fe I 1565 nm

Impressive splitting at 12 micron.

De Wijn (2012)

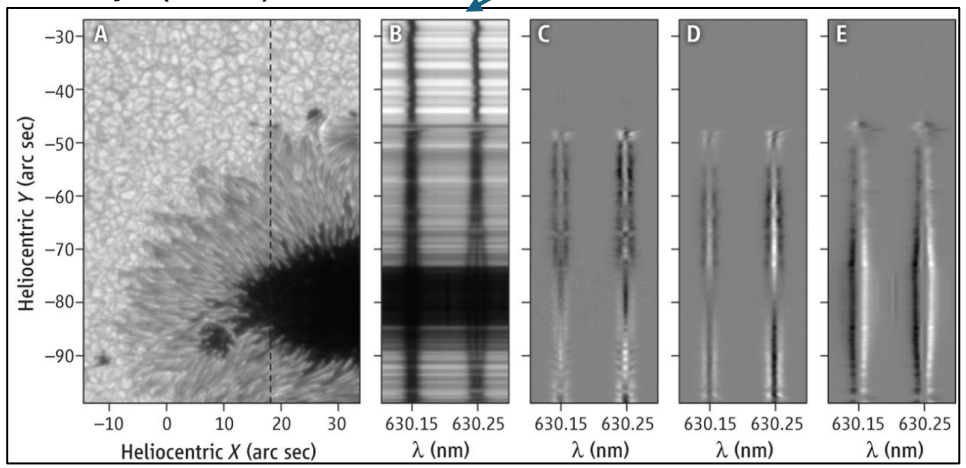

Hinode/SP 630 nm

Penn (2004a)

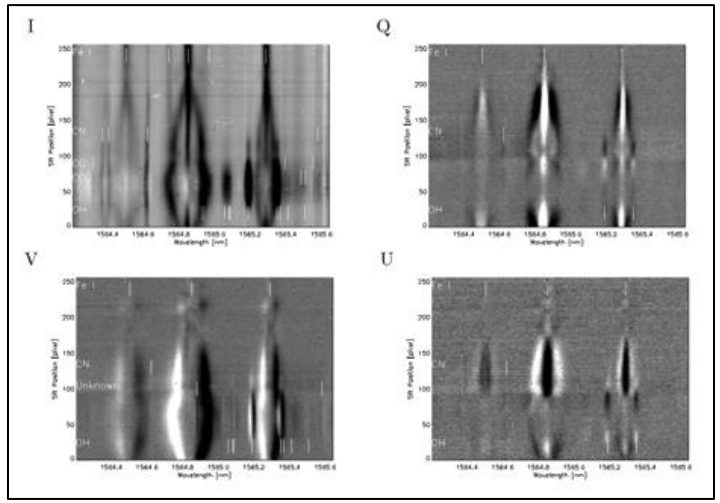

Example spectra from the McMath/Pierce

Moran et al. (2000)

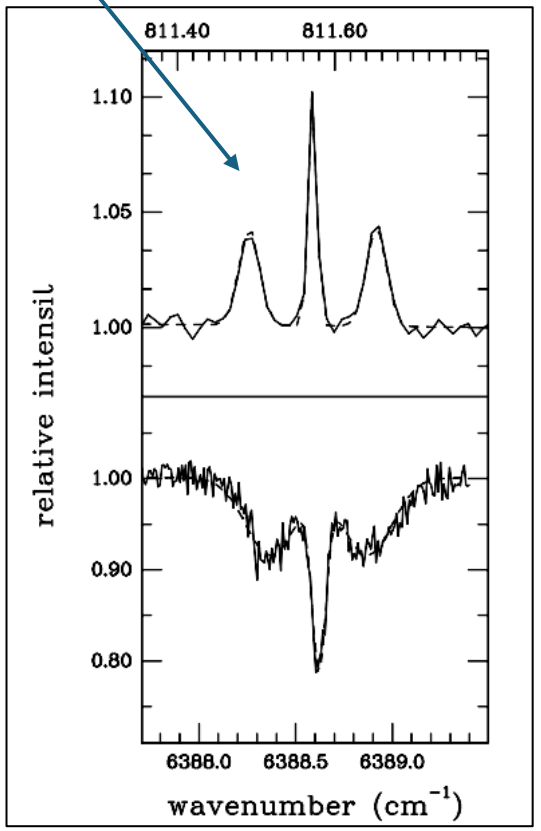

Mg I 12318 nm

Fe I 1565 nm

Fe I 1565 nm is now a key diagnostic line of DKIST/DL-NIRSP, NST/NIRIS, GREGOR/GRIS.

IR Atomic Lines: The Neutral Helium Triplet

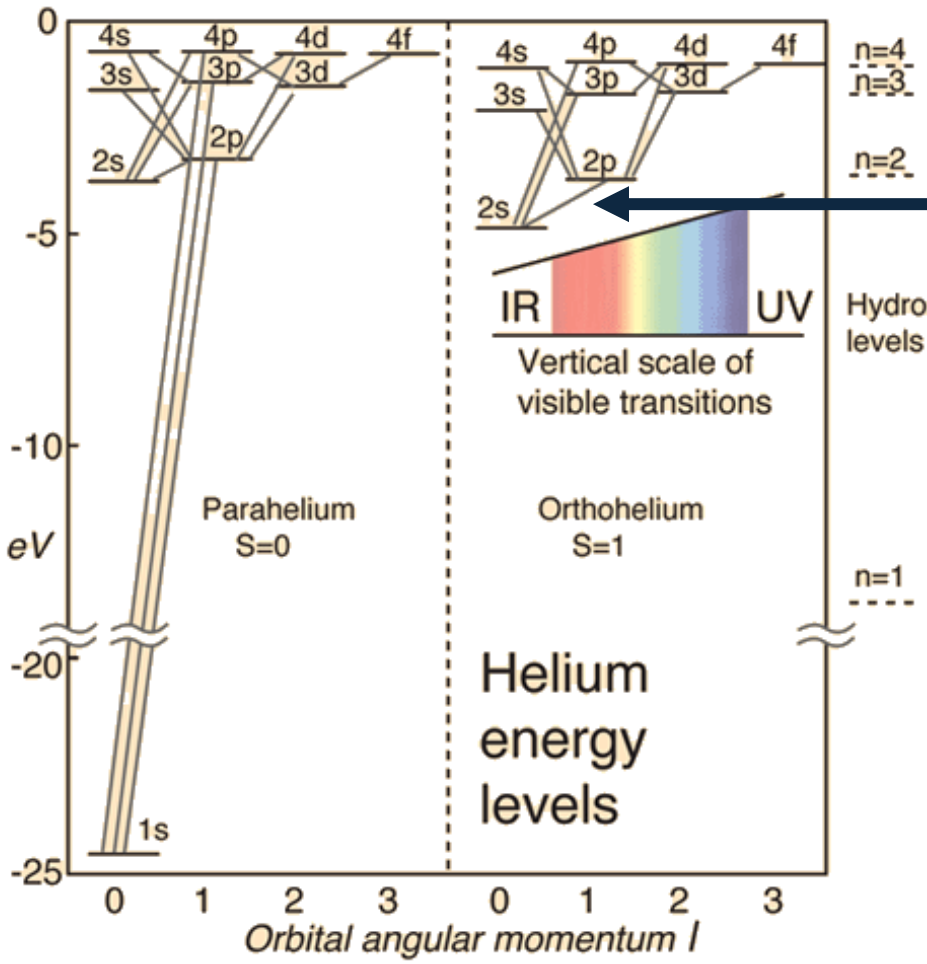

Image credit:Hyperphysics

He I 1083 nm

A very valuable line for solar chromospheric and TR physics.

The triplet state of neutral helium has a metastable ground level.

Non-LTE:
Photoionization (λ<504 Å) and recombination largely populates triplet.

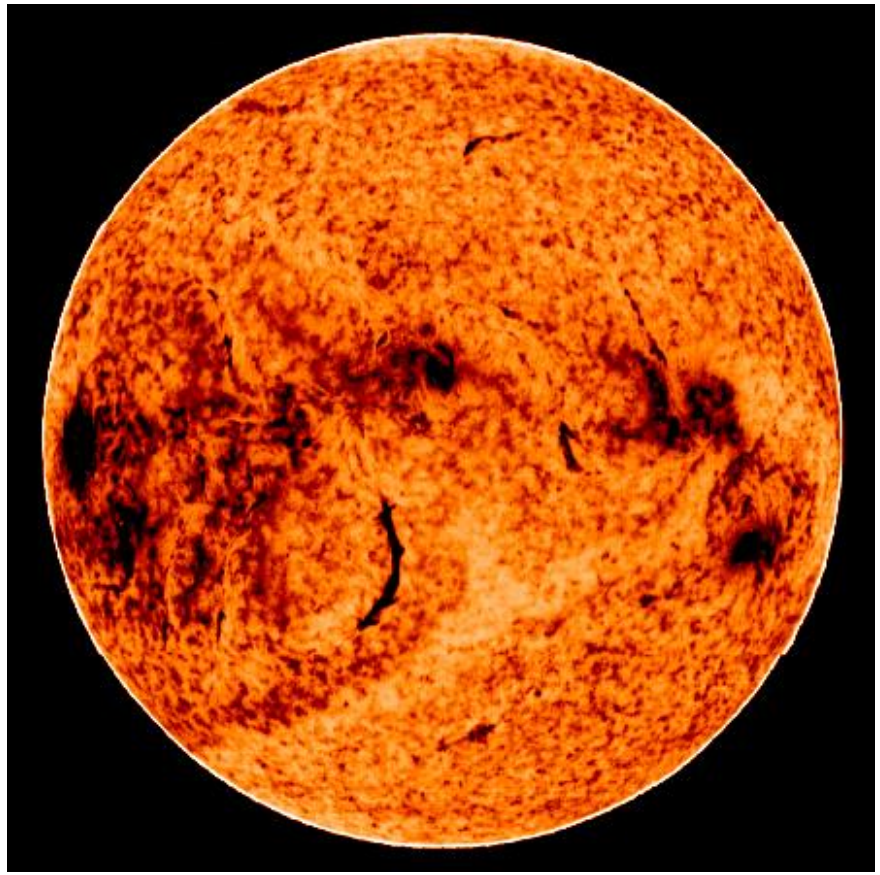

Kitt Peak He I Spectroheliogram (27 June 1998)

* Pronounced absorption for hot active regions and dense filaments.
* Very weak in coronal holes.

IR Atomic Lines: The Neutral Helium Triplet

Asensio Ramos et al. (2008)

TABLE 1

He I Atomic Data

Transition ($u \rightarrow l$)	Air wavelength (Å)	$A(\beta_u L_u S J_u \rightarrow \beta_l L_l S J_l)$ (s^{-1})	B^{up}_{crit} (G)
$2p\ ^3P_0 – 2s\ ^3S_1$	10829.0911	1.022×10^7	Undefined
$2p\ ^3P_1 – 2s\ ^3S_1$	10830.2501	1.022×10^7	0.77
$2p\ ^3P_2 – 2s\ ^3S_1$	10830.3398	1.022×10^7	0.77

- He I 1083 consists of 3 transitions
- Atomically polarized by optical pumping by the anisotropic illumination of the lower atmosphere.
- Collisional rates too low to depolarize permitted transitions.
- Sensitive to Hanle effect up to ~ 8 G (~10x B_{crit}).
- Zeeman + Paschen Back effects at large field strengths.

Trujillo Bueno et al. (2002)

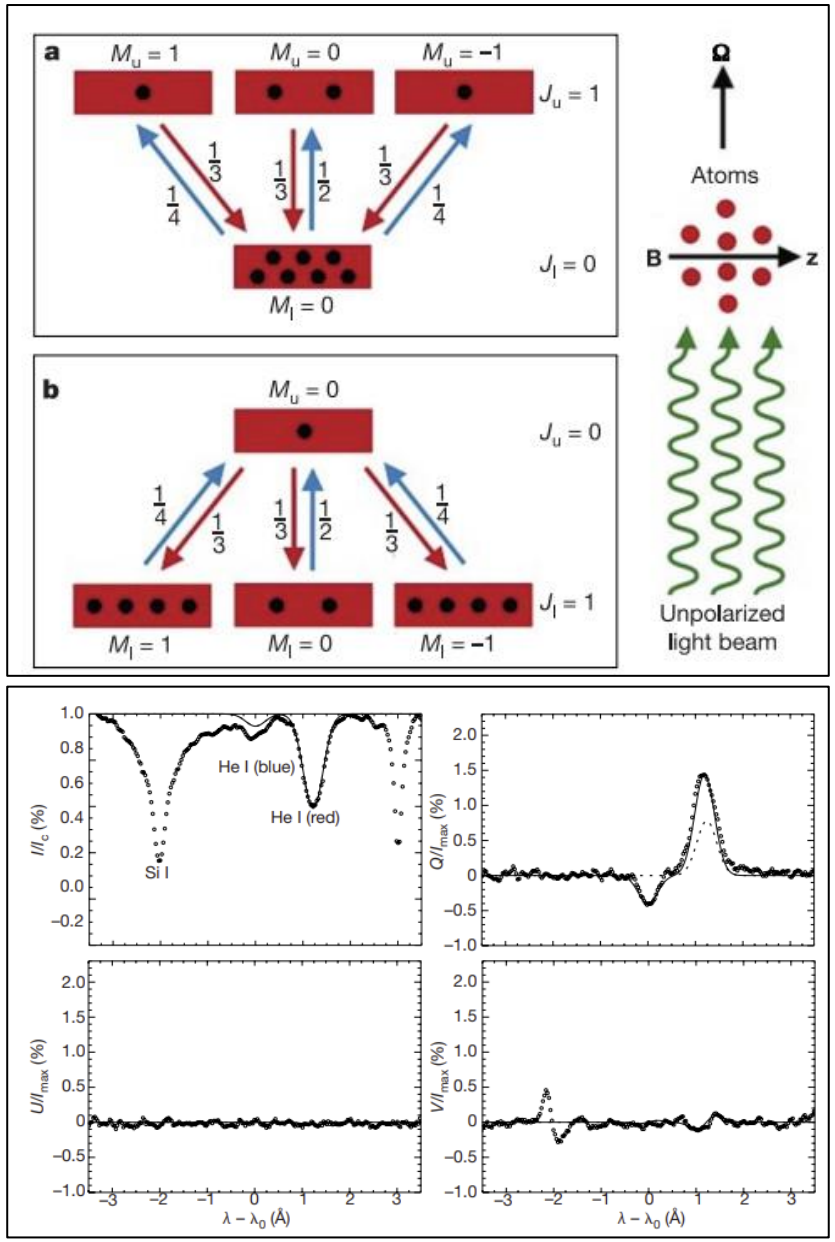

IR Atomic Lines: The Neutral Helium Triplet Active Region Polarization

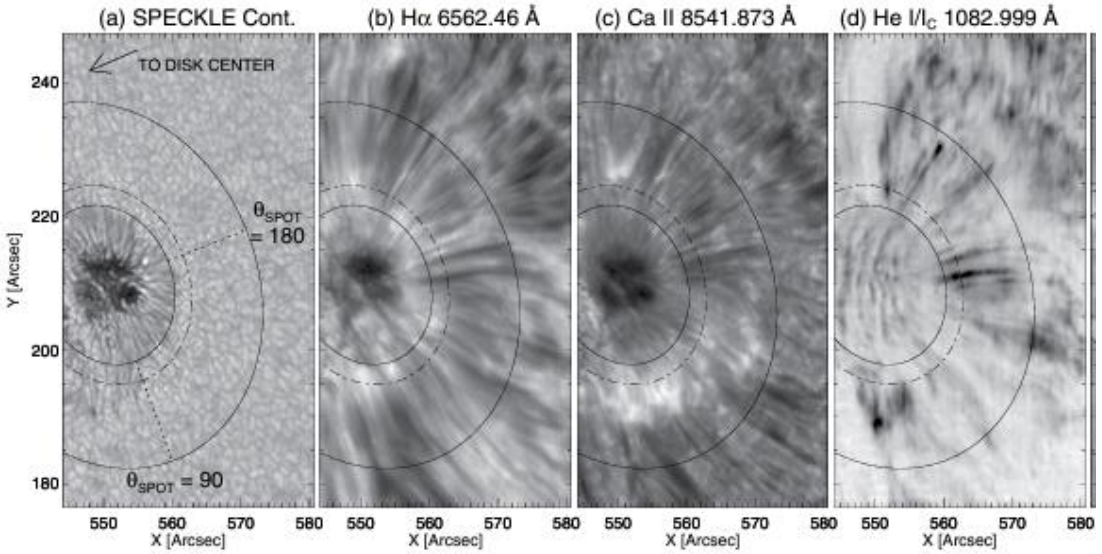

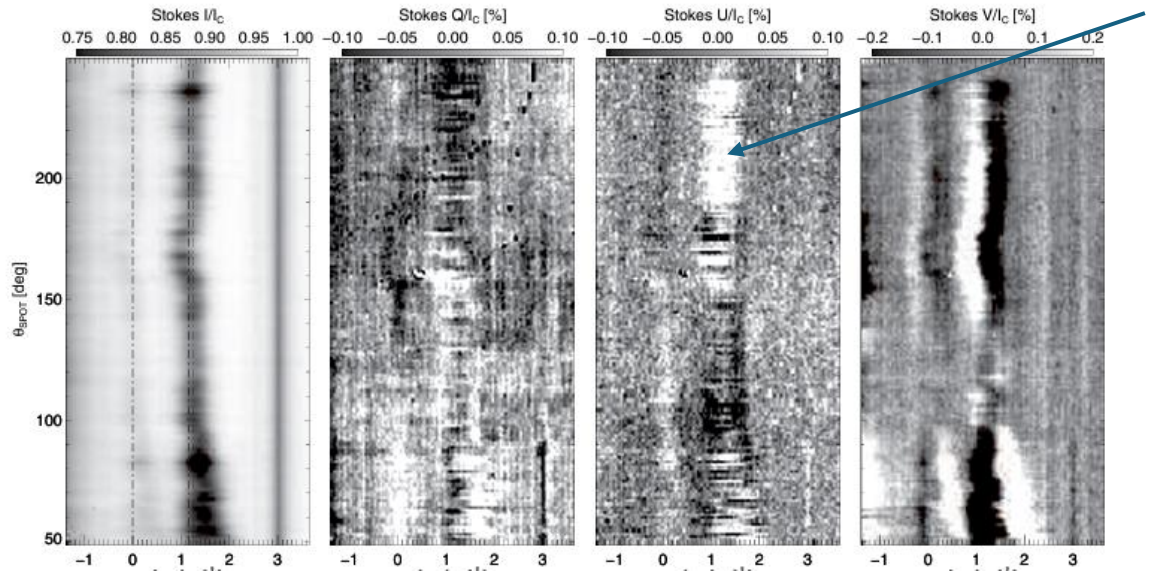

Schad et al. (2013)
Superpenumbral fibril magnetic fields

Zeeman dominated signals within umbra.

Scattering polarization signals outside of umbra, which is responsible for sign flip of line center polarization for red transition and not the lower-level polarization dominated blue component.

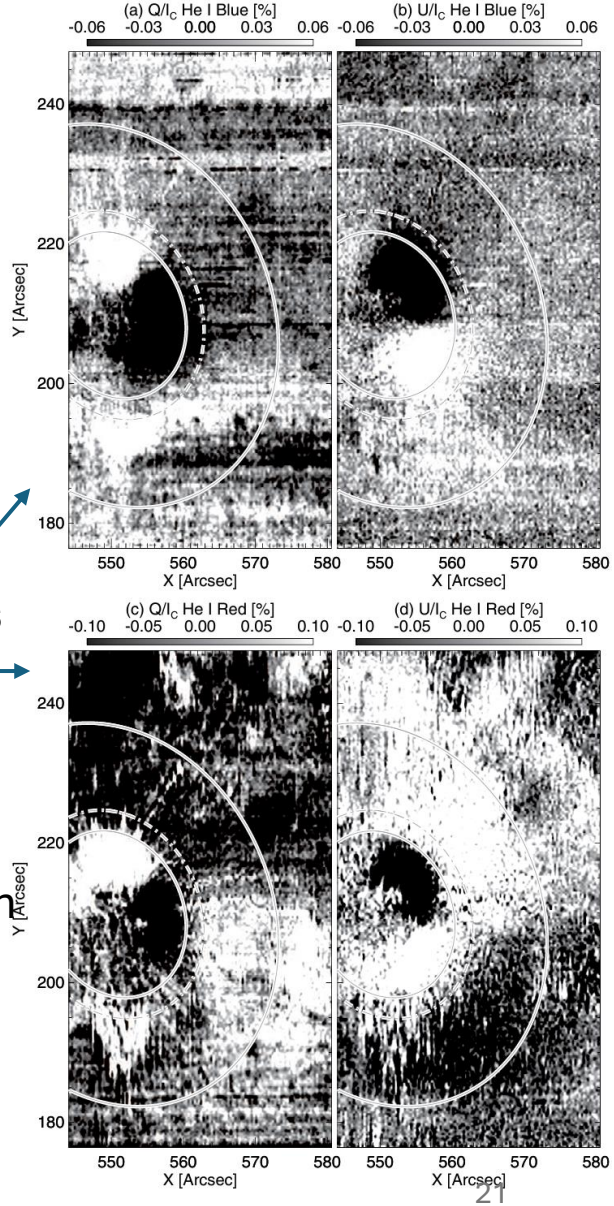

Infrared Molecular Lines

- Molecular energy transitions (vibration and rotations) occur at lower energies than atomic electron transitions.
- Leads to more molecular transitions in the IR, as is clear given the telluric absorption.

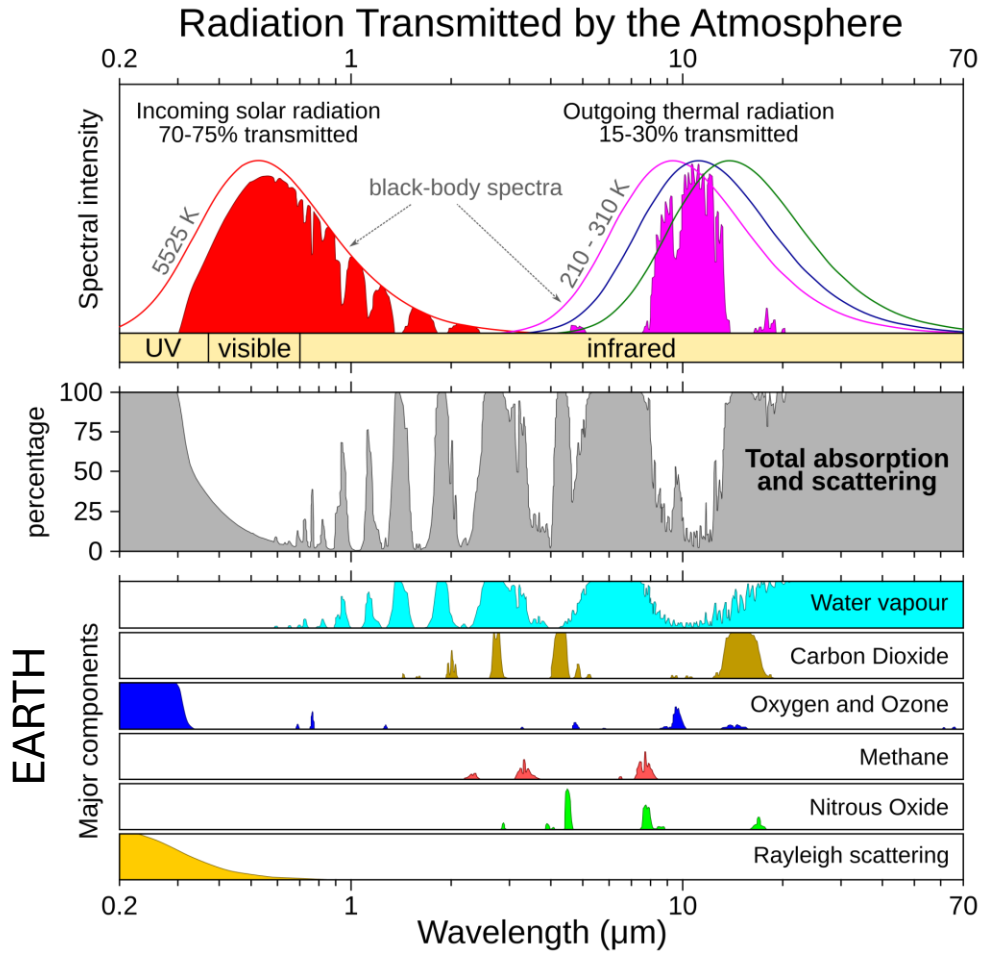

Berdyugina et al. (2003)

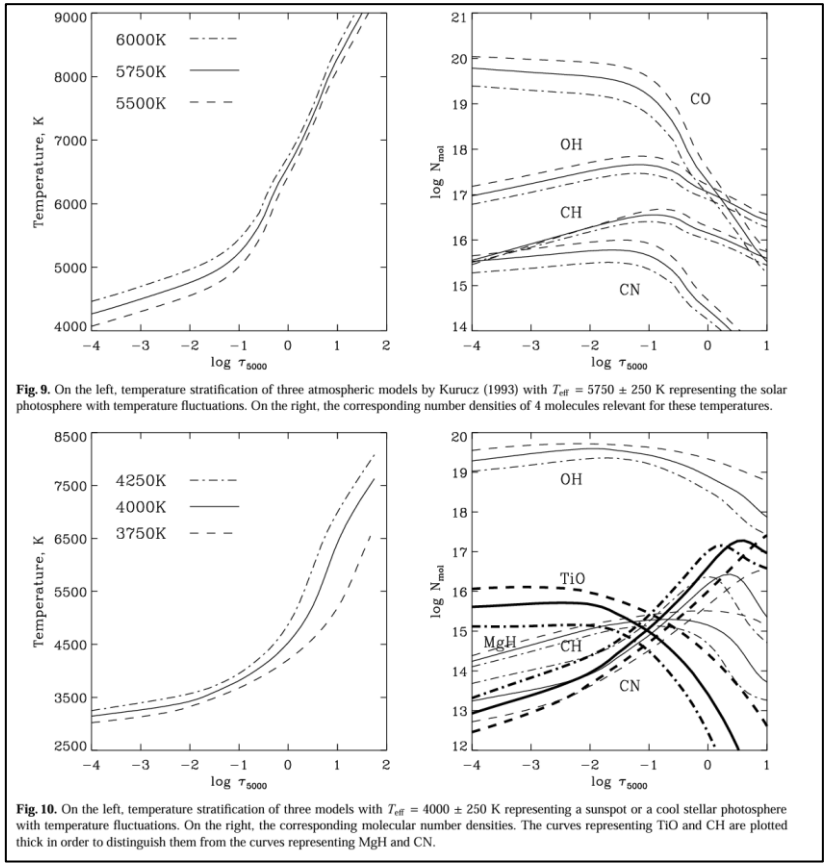

Quiet Sun

Key solar species include diatomic molecules of C, O, H, N

Umbra

OH bands near 1.6 and 3.5 um.

Infrared Molecular Lines

- Molecular energy transitions (vibration and rotations) occur at lower energies than atomic electron transitions.
- Leads to more molecular transitions in the IR, as is clear given the telluric absorption.

Sanchez Almeida et al. (2001)

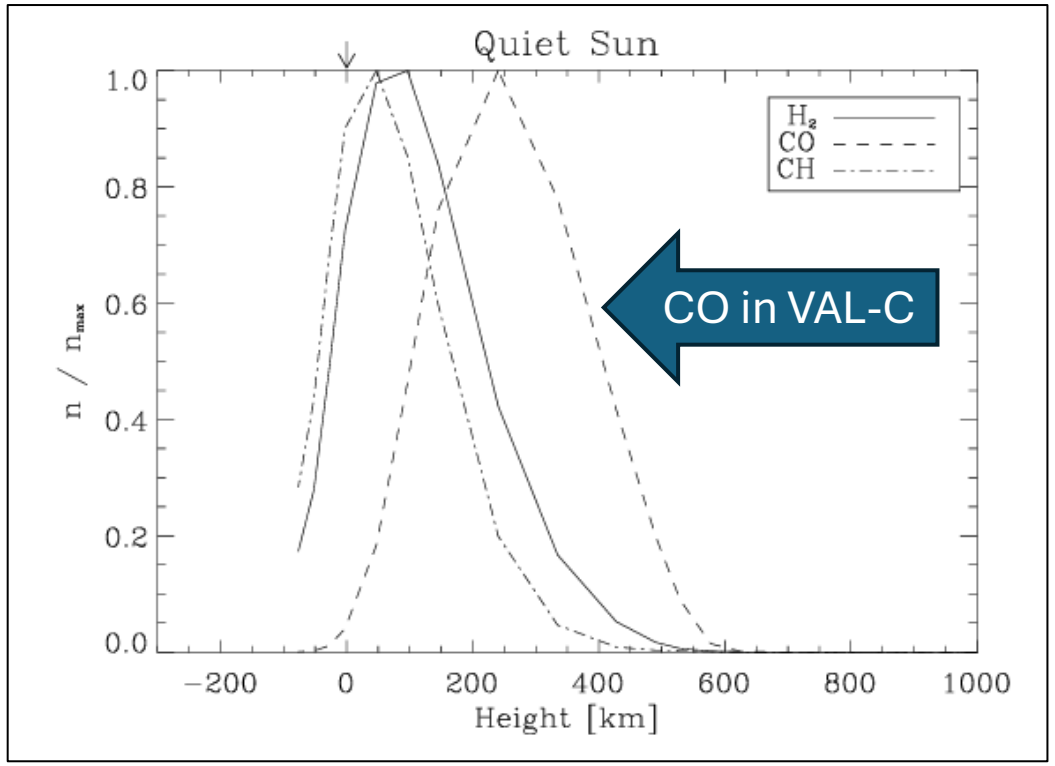

Carbon monoxide is particularly important. Most abundant after H2 due to high dissociation energy.

Berdyugina et al. (2003)

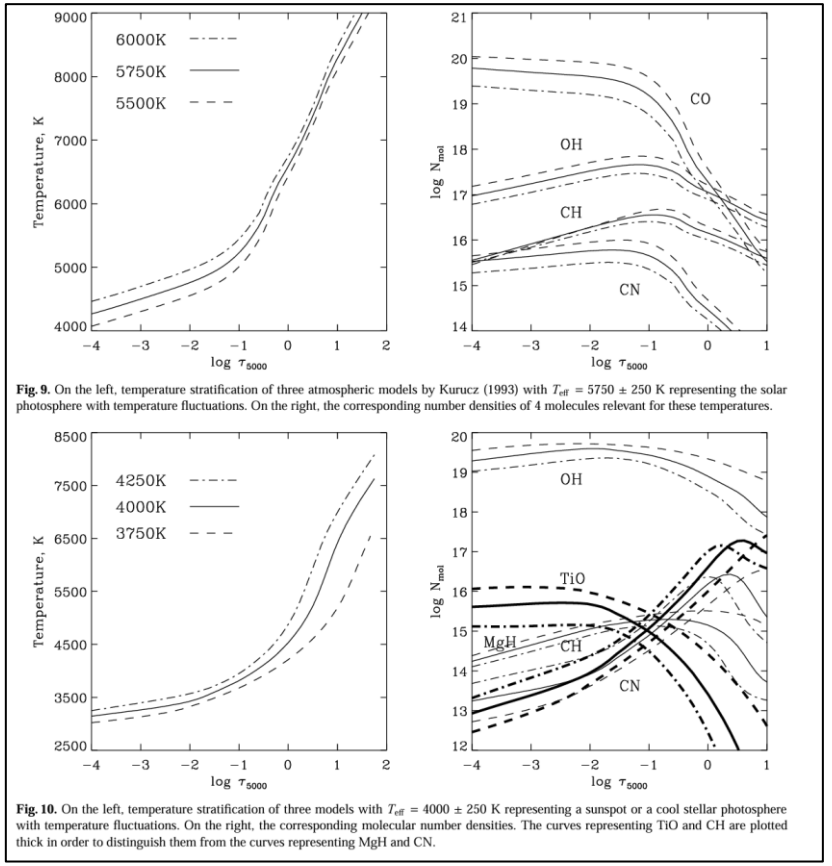

Quiet Sun

Key solar species include diatomic molecules of C, O, H, N

Umbra

OH bands near 1.6 and 3.5 um.

Infrared Molecular Lines: Carbon Monoxide

- Noyes & Hall (1972); Ayres & Testerman (1981):
  - Cool **(T ~3500 K)** CO clouds in solar atmosphere.
- Cool material and low degree of ionization important to model ambipolar diffusion and field slippage
- Many numerical models (e.g., BiFROST) enforce artificial lower temperate boundary.
- See recent work by CU-Boulder graduate J. Stauffer

J.T. Jefferies (1994)

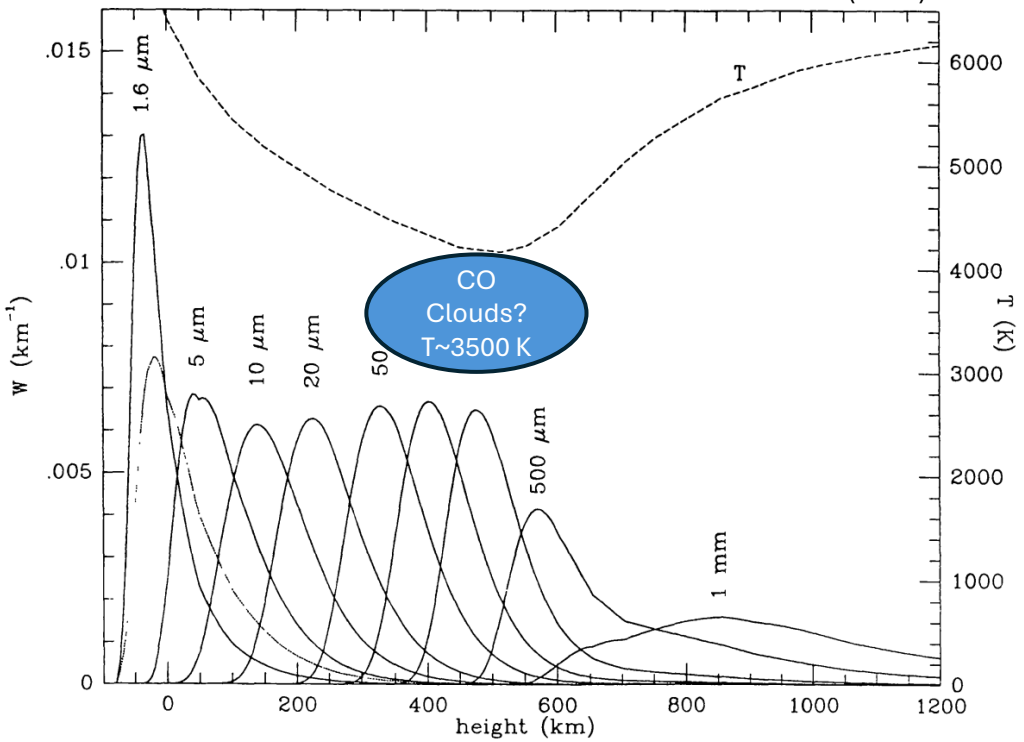

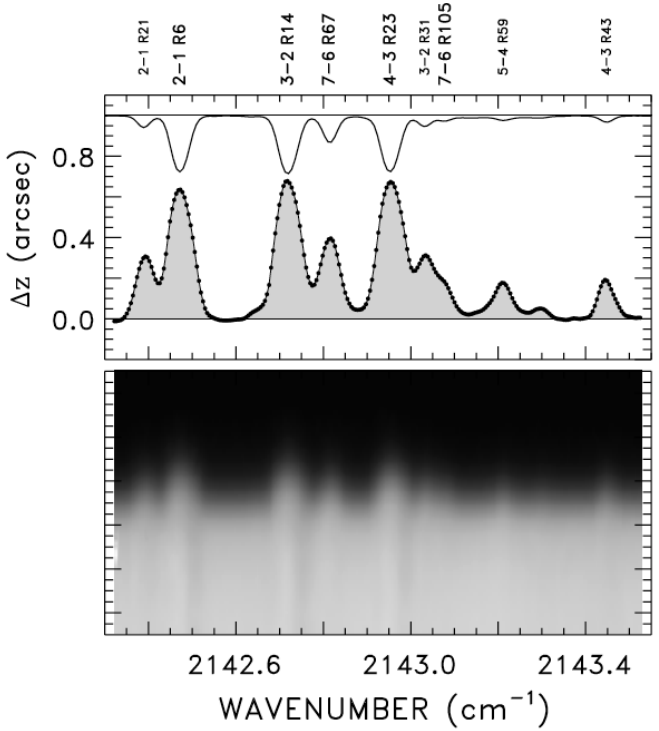

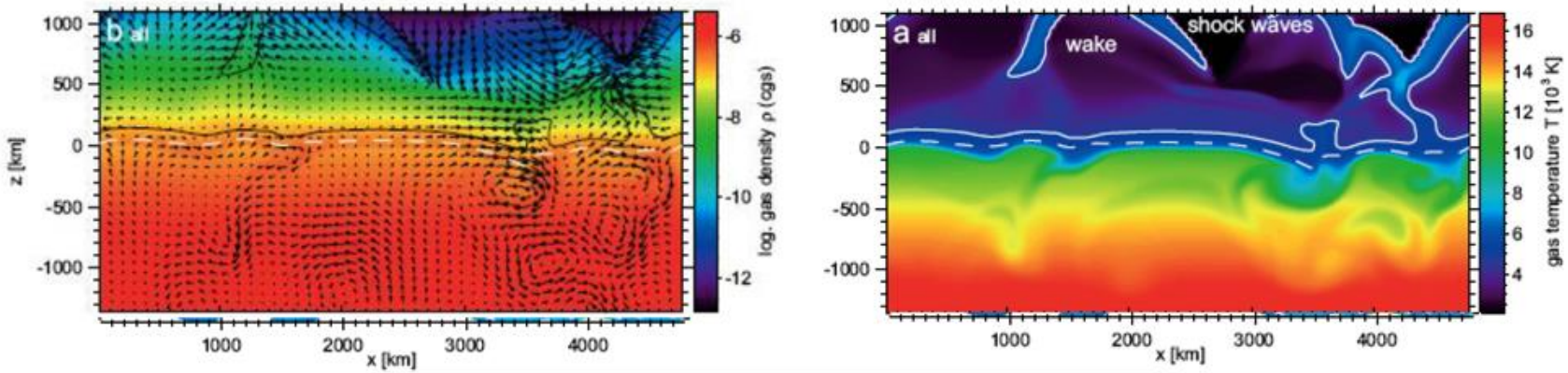

Wedemeyer-Böhm et al. 2005, A&A 438, 1043

Infrared Coronal Emission

- The enduring mystery of the solar corona started with observations of visible coronal continuum (Thomas scattering by elections) and line emission from highly ionized lines.
- Limited to solar eclipses due to the bright solar disk at visible and infrared wavelengths.
- Compared to solar disk continuum intensity, visible/IR emission is ~(1-100) : 10^6
- Why observed them at all?

Some key advantages include:

1. Photoexcited emission (Thomson scattering and Vis/IR lines) is brighter at more extended elongations.
2. Anisotropic photoexcitation → polarized lines in saturated Hanle effect.
3. Long wavelength → possibility to measure Zeeman effect magnetic field.

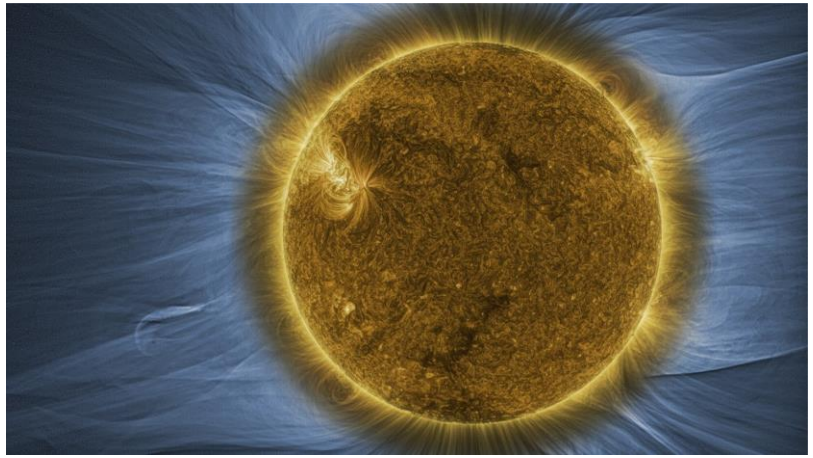

Image credit: UH/Habbal/Druckmuller SDO/AIA

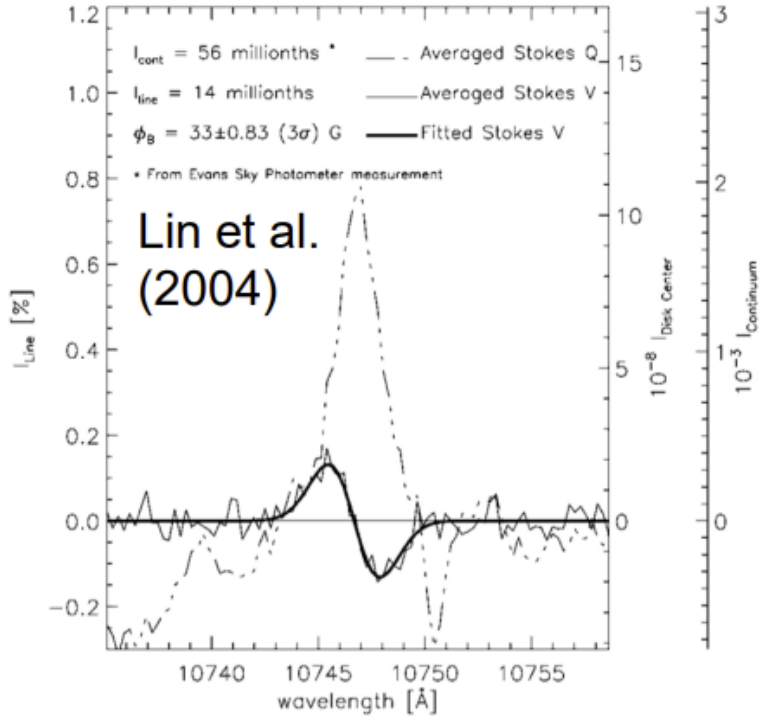

Infrared Coronal Emission Lines: Spectral observations

- Incomplete exploration and atomic data make IR lines a big discovery space (del Zanna & DeLuca (2017) review)
- Mostly observed during eclipses.
- HAO CoMP (UCoMP) observes Alfvenic waves in Fe XIII 1074 nm line + linear polarization coronagraphically.
- DKIST large aperture coronagraphy in progress.

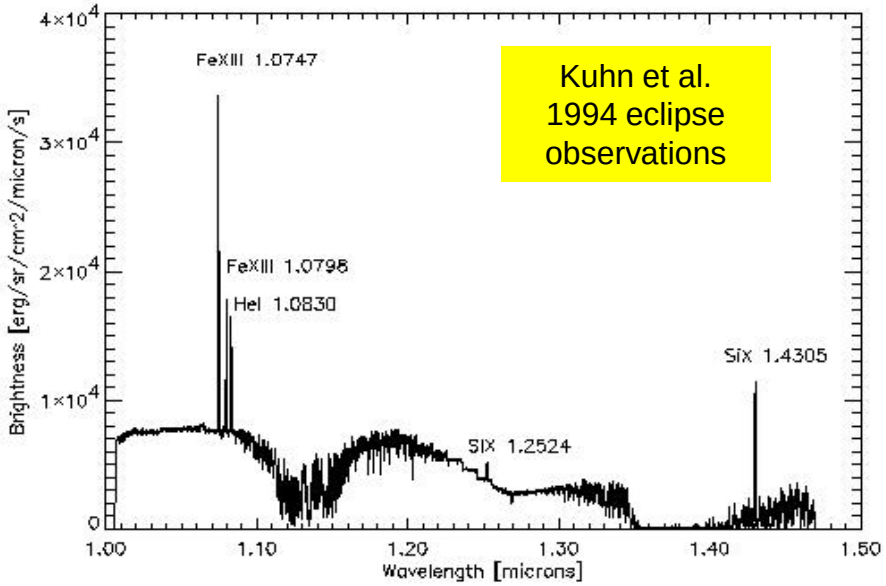

Kuhn et al. 1994 eclipse observations

Tomcyzk et al. (2007); Tomczyk and McIntosh (2009)

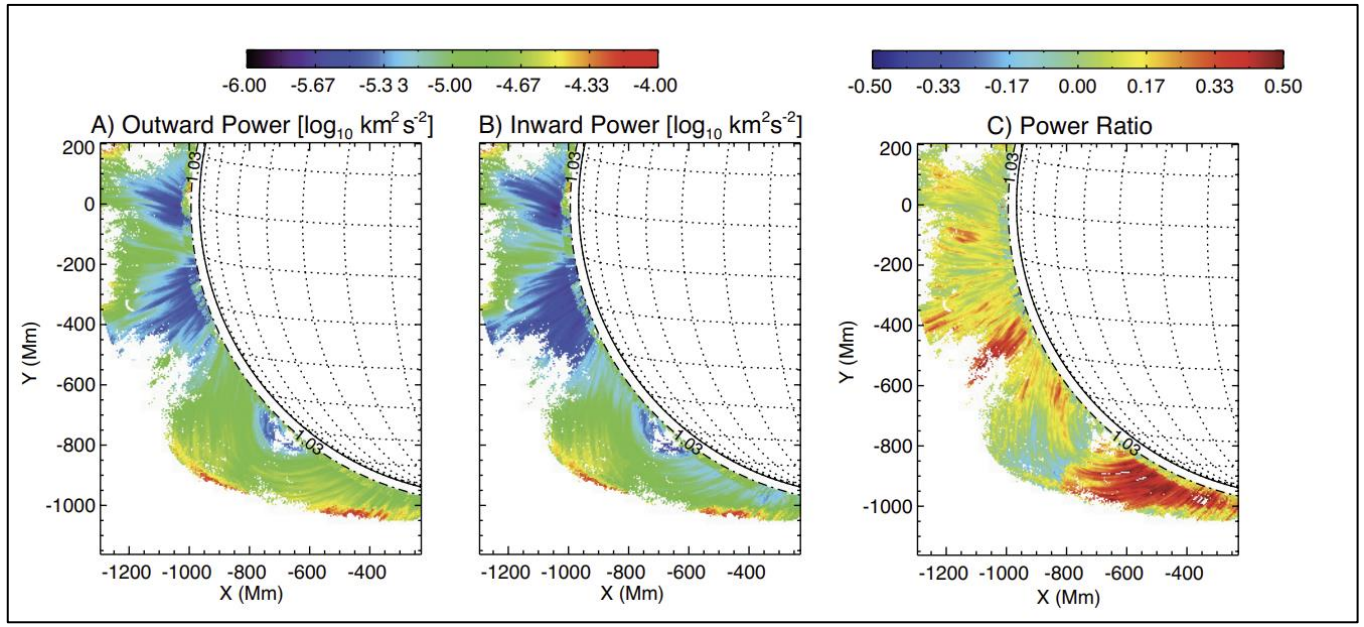

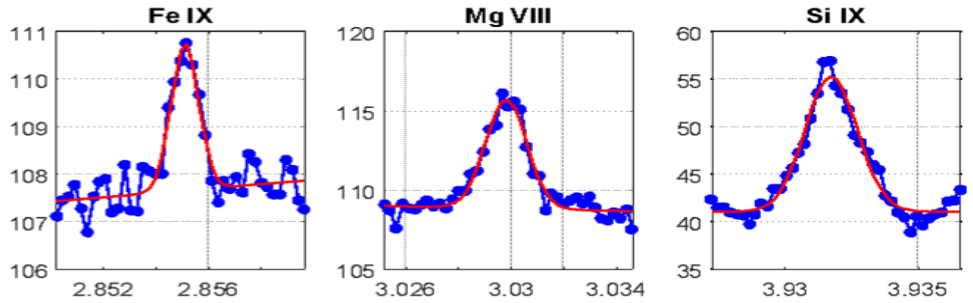

SAO *Air-Spec* 2017 Eclipse Observations

Courtesy of Jenna Samra and Ed DeLuca

Infrared Coronal Emission Lines: New polarimetric results from DKIST

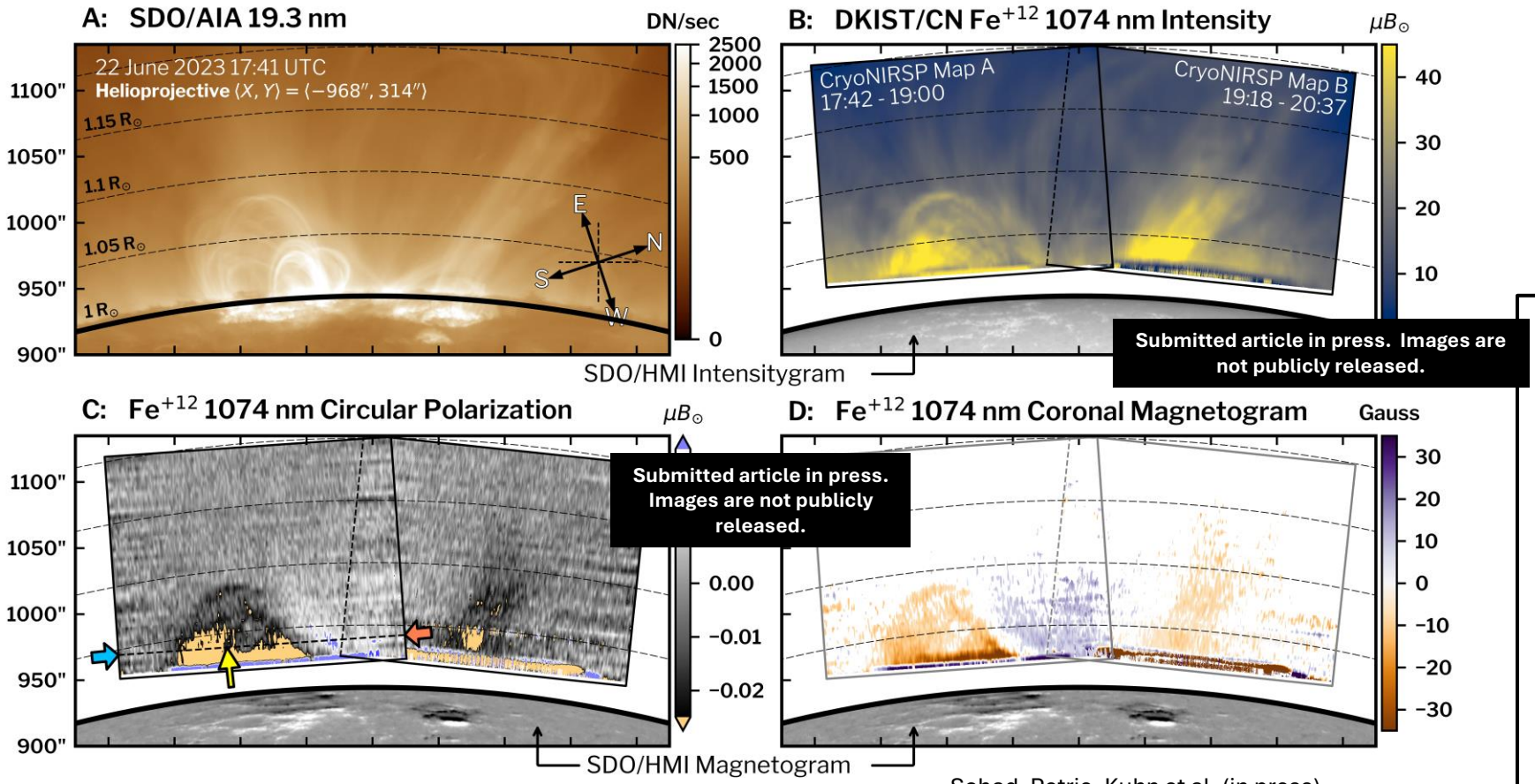

Submitted article in press. Images are not publicly released.

Submitted article in press. Images are not publicly released.

Units: μB ==> ppm of disk radiance ==> 'millionths'

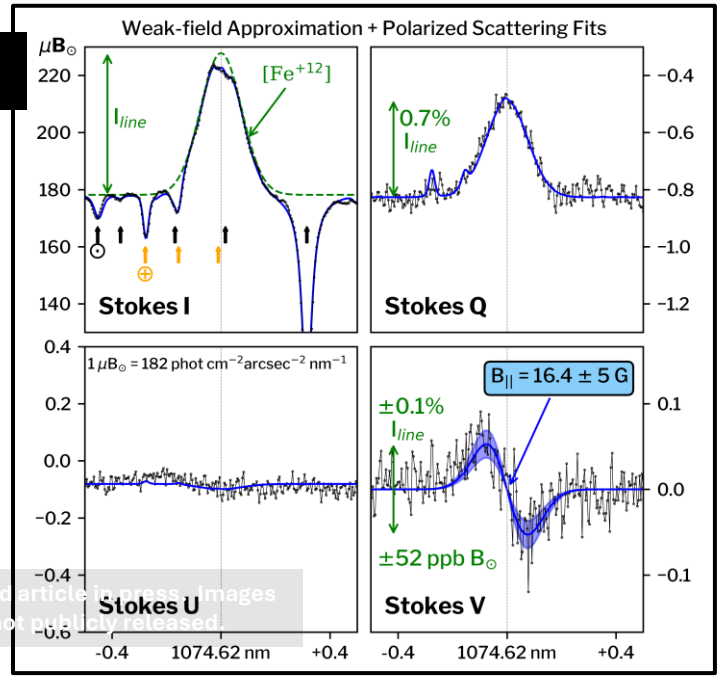

Schad, Petrie, Kuhn et al. (in press)

Submitted article in press. Images are not publicly released.

This afternoon we will work with some of the DKIST/CryoNIRSP spectroscopic data from the corona and discuss line emission calculations.

Lecture Outline

- Defining the Infrared: A short history
- The Infrared Solar Spectrum
  - Continuum formation and flare emission
  - Atomic lines of the lower atmosphere
  - Molecular species
  - Coronal emission
- **Observing at Infrared Wavelengths**
  - Advantages and disadvantages
  - Detectors
  - Optics
  - Cryostats
  - Coronagraphs
- Summary and Outlook
  - This afternoon's tutorial: Coronal IR Spectroscopy using DKIST/CryoNIRSP

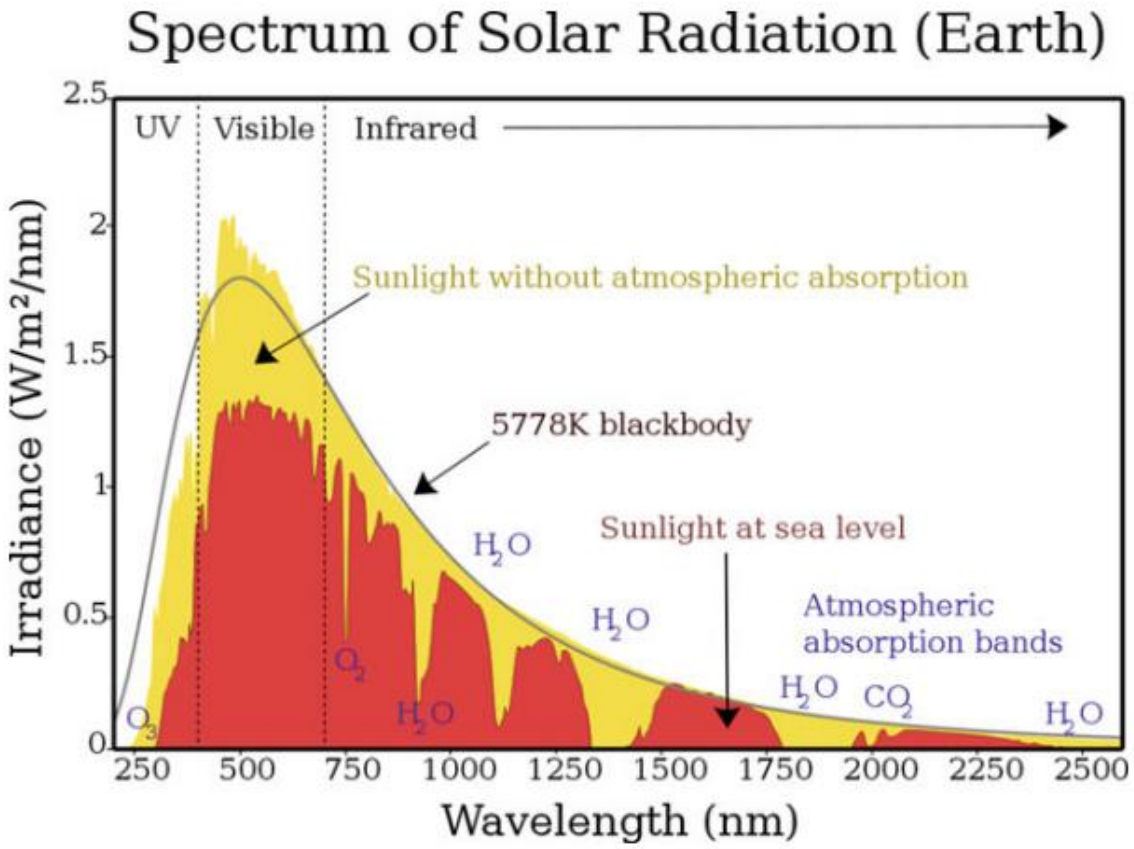

Infrared Solar Physics: Advantages and Disadvantages

Harvey and Hall (1971) ; Penn (2014)

Advantages	Disadvantages
Increased Zeeman resolution	Fewer atomic absorption lines
Large number of molecular rotation-vibration lines	Larger diffraction limit**
Ability to probe different heights in the solar atmosphere using continuum radiation	Increased thermal background
Smaller instrumental polarization	Fewer solar photons*
Less instrumental scattering	Detector complexities
Less atmospheric scattering	More limited optical transmissive materials (i.e. can require more complex powered mirrors)
Better atmospheric seeing [Fried $r_0 \sim \lambda^{6/5}$]	**Atmospheric telluric absorption**

** Note collecting area increases as D^2 whereas the diff. limit decreases as D^{-1}. Large aperture boosts value of IR science

Infrared Solar Physics: Earth's Atmosphere Transmission Spectrum

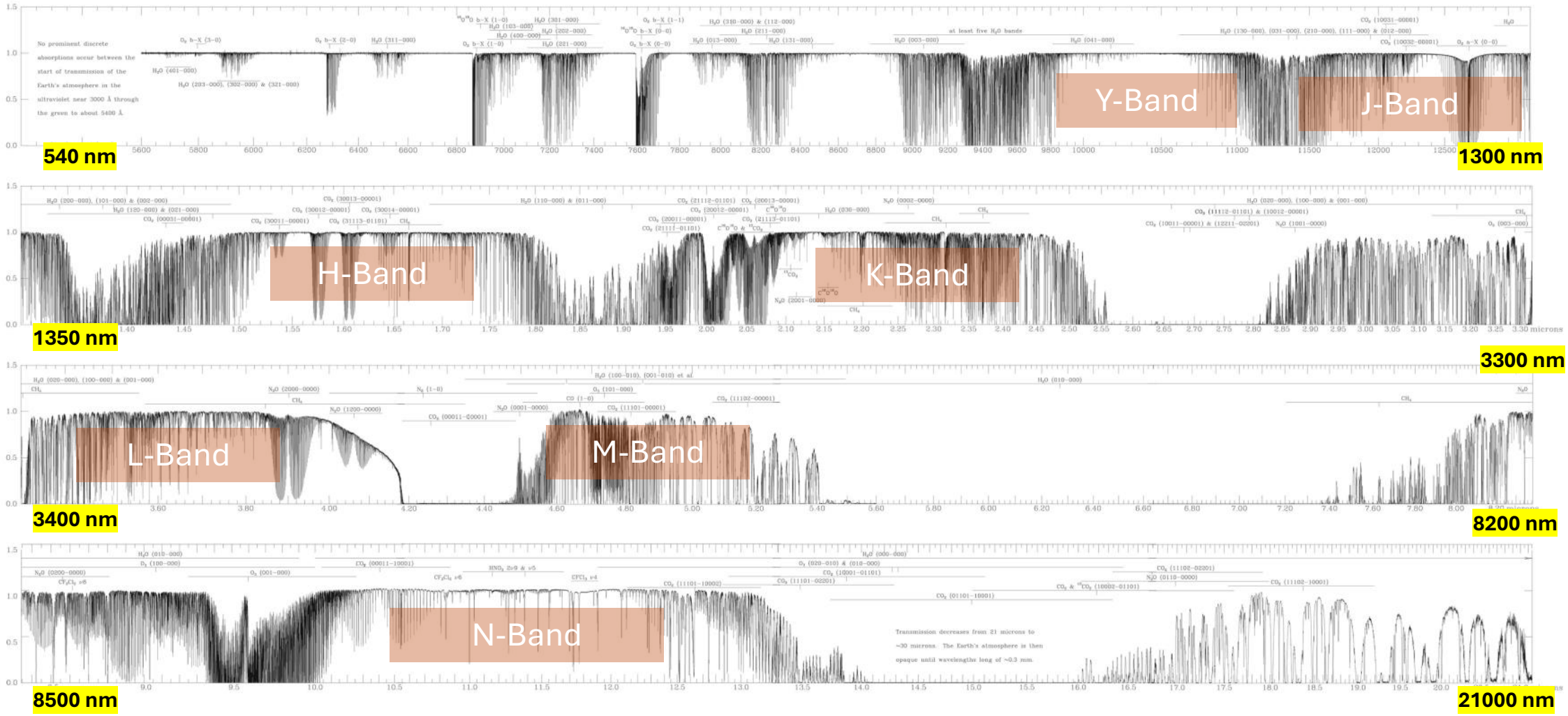

Figure 1: Atmospheric transmission from 560 to 21 000 nm as measured from the McMath–Pierce facility at Kitt Peak. The molecules which are responsible for the various absorption bands are marked. Image reproduced with permission from Hinkle *et al.* (2003), copyright by AAS.

IR Solar Physics: Telluric Absorption near CO fundamental band.

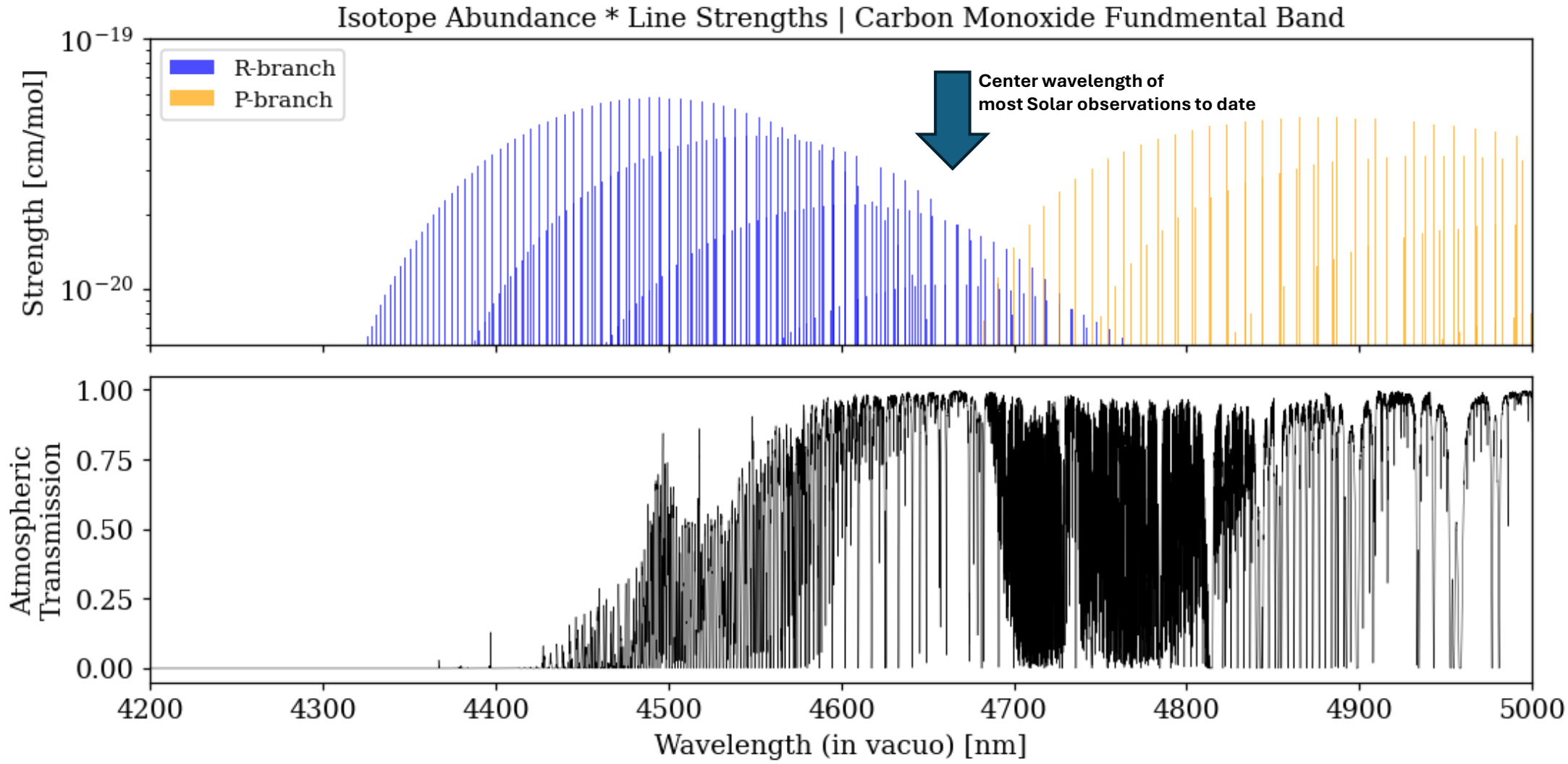

IR Solar Physics: Telluric Absorption near coronal lines.

Coronal Emission Line

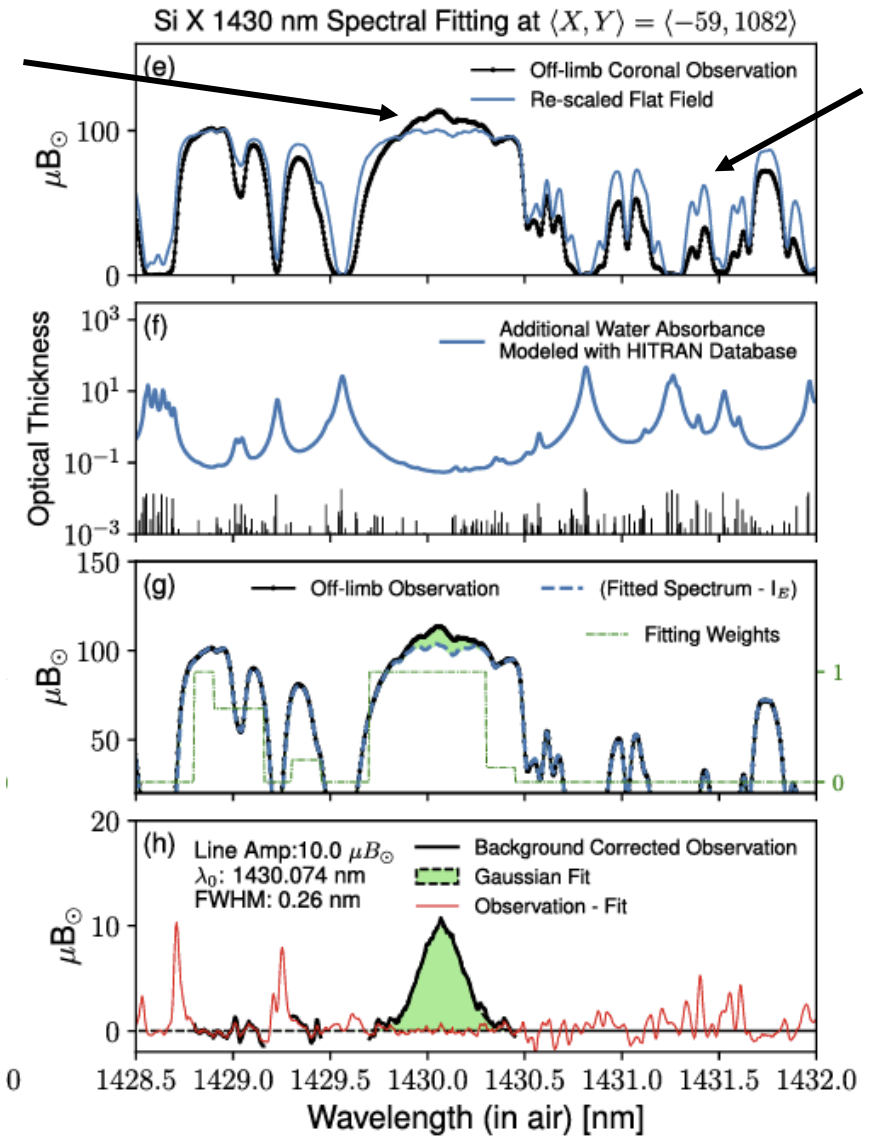

Schad et al. (2024)

CO_2 + H_20

telluric bands

NO_2

telluric bands

Spectroscopy requires developing methods to treat telluric +scattered light + other systematics

Coronal Emission Line

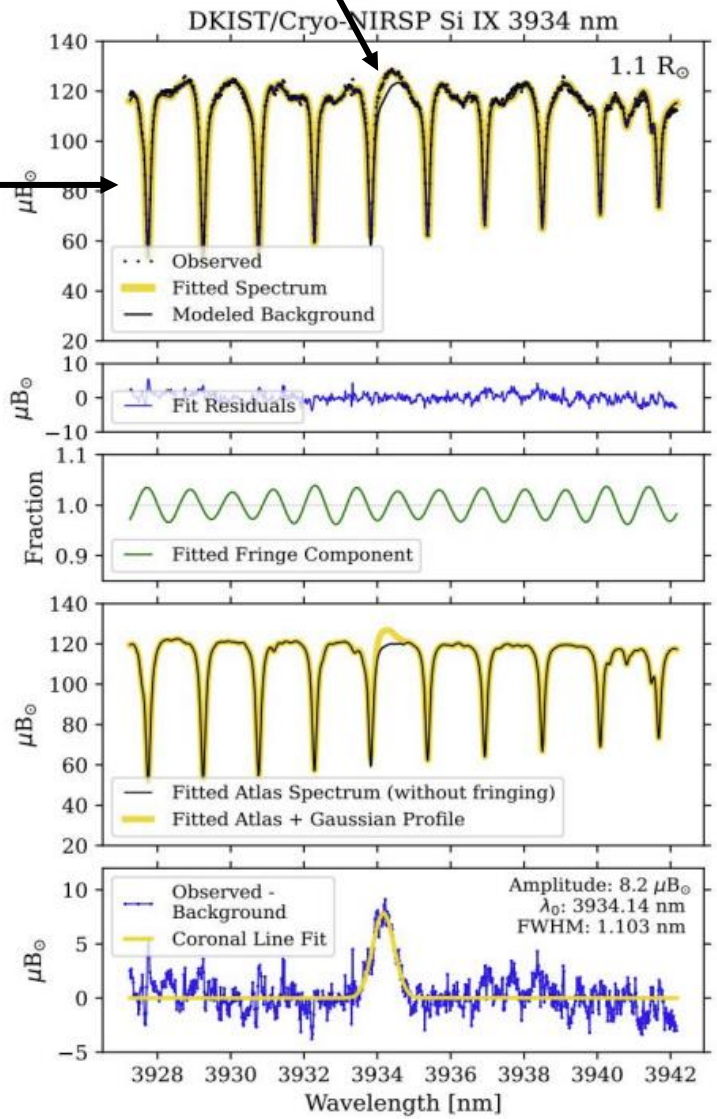

Schad et al. (2023)

Infrared Solar Physics: Advantages and Disadvantages

Harvey and Hall (1971) ; Penn (2014)

Advantages	Disadvantages
Increased Zeeman resolution	Fewer atomic absorption lines
Large number of molecular rotation-vibration lines	Larger diffraction limit**
Ability to probe different heights in the solar atmosphere using continuum radiation	Increased thermal background
Smaller instrumental polarization	Fewer solar photons*
Less instrumental scattering	**Detector complexities**
Less atmospheric scattering	More limited optical transmissive materials (i.e. can require more complex powered mirrors)
Better atmospheric seeing [Fried $r_0 \sim \lambda^{6/5}$]	Atmospheric telluric absorption

** Note collecting area increases as D^2 whereas the diff. limit decreases as D^{-1}. Large aperture boosts value of IR science

Infrared Detectors: Major Sensor Materials

Silicon is the dominant material used short of ~ 900 nm.

The range of infrared materials used is broad and evolves as the material science and fabrication techniques develops.

HgCdTe (“Mer-Cad-Tel”) is dominant for astronomical imaging applications due to:

- Large λ sensitivity range
- Tunable bandgap.
- Large array sizes possible

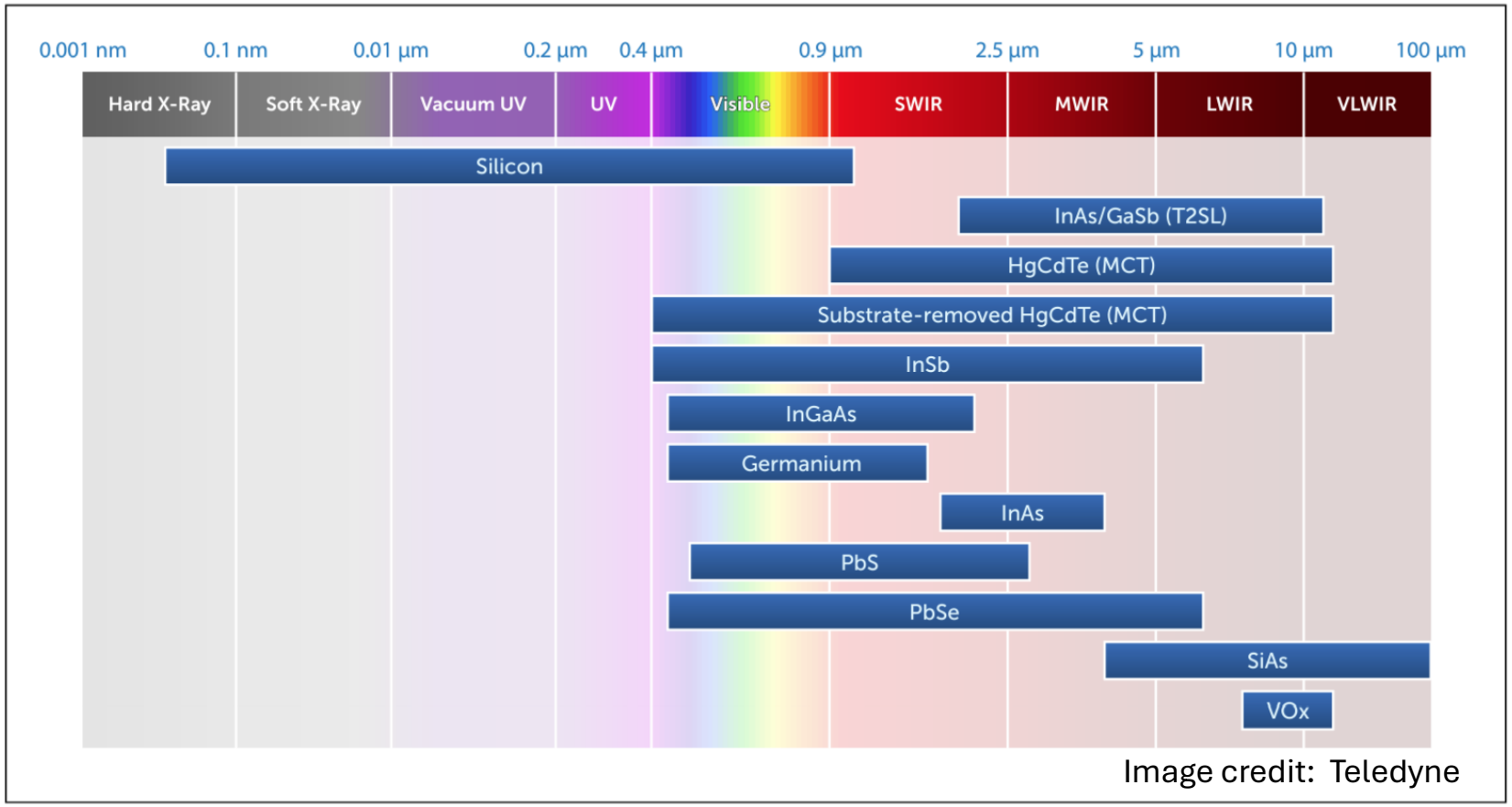

Image credit: Teledyne

Infrared Detectors: FPA development and sizes and pitch

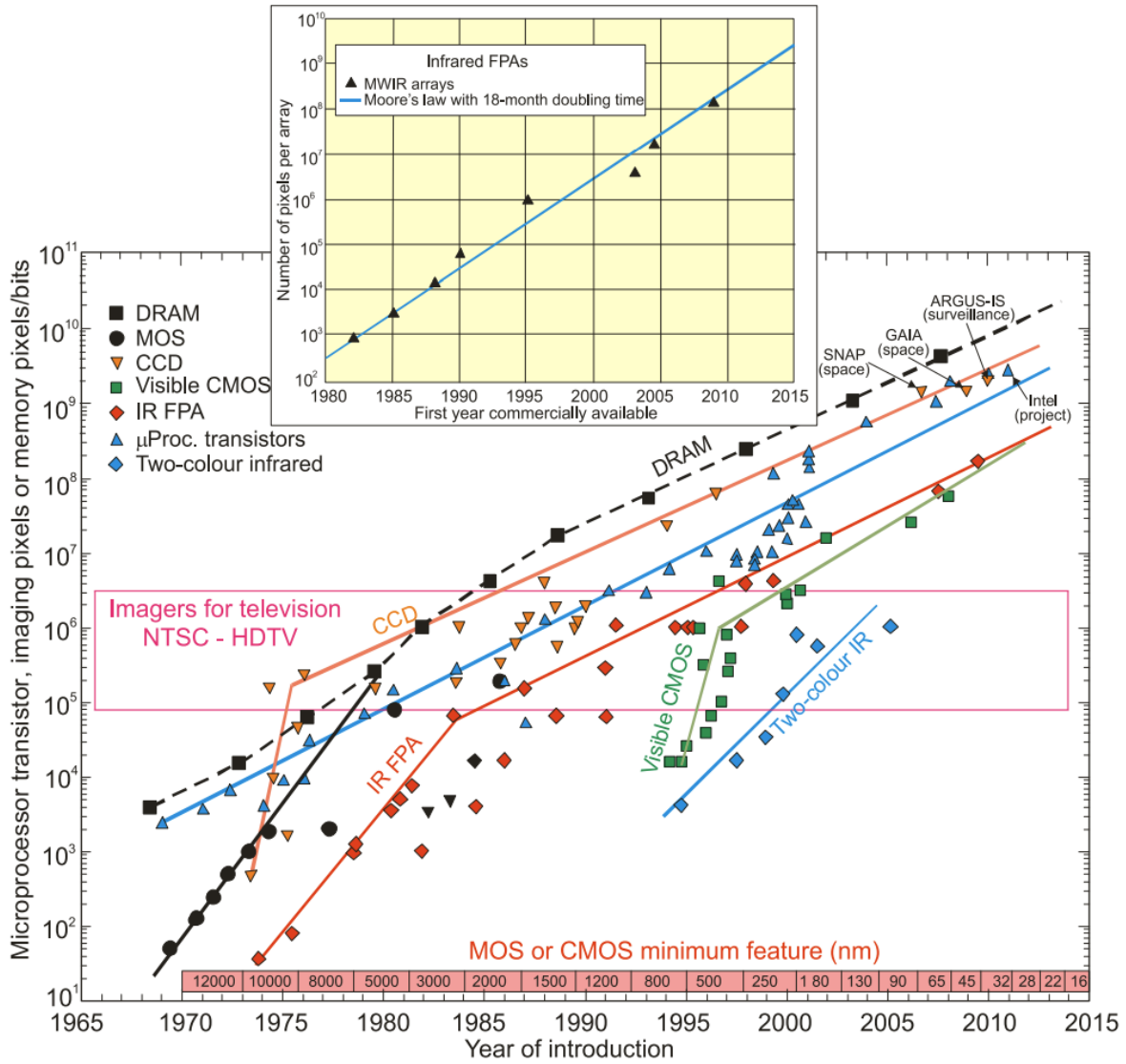

Rogalski (2012)

FPA: "Focal plane array"

Infrared materials need to be bonded to silicon ROICs.

EUV lithography standard size is 23 x 33 mm, which can limit the size of continuous arrays.

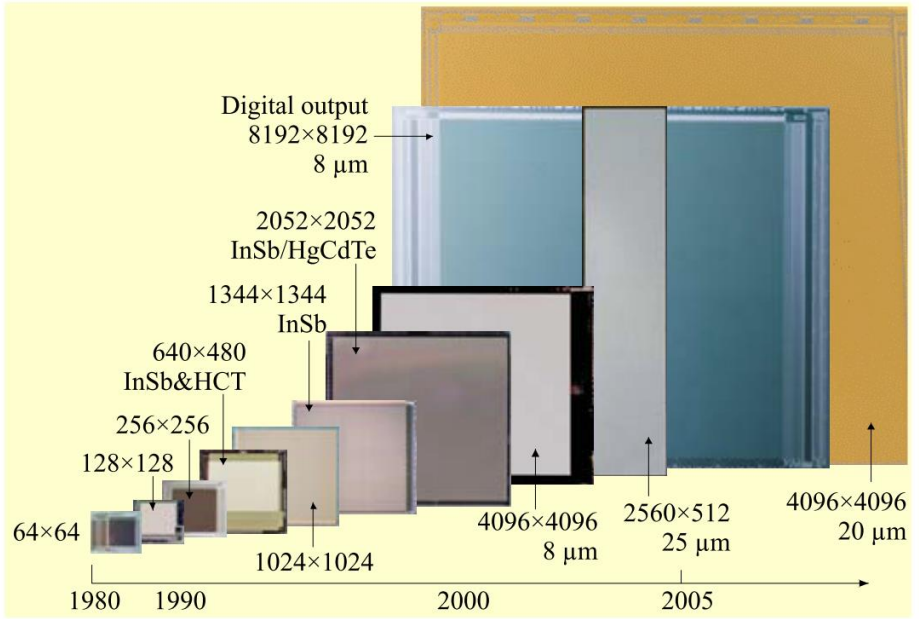

Fig. 30. Progression of ROIC format at RVS over time (after Ref. 96).

Infrared Detectors: Unique sampling modes for measurements

"Up-the-ramp" Sampling

How it works: The H2RGs individual pixel charges can be read non-destructively (i.e. the charge is not reset until the end of a sequence). So, some regions of the array can be allowed to saturate while the integration continues up the well.

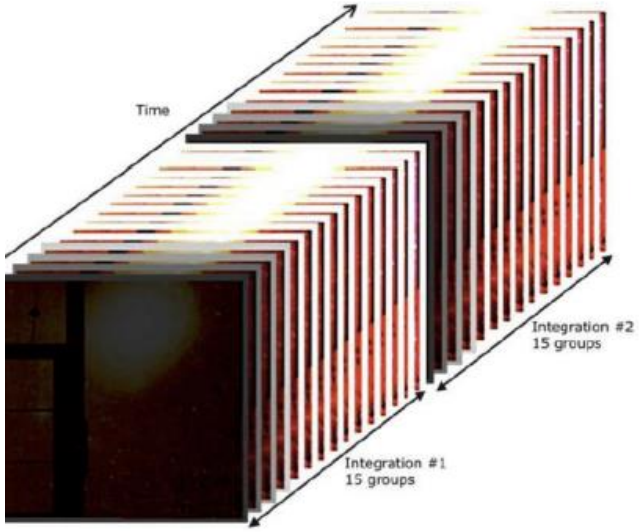

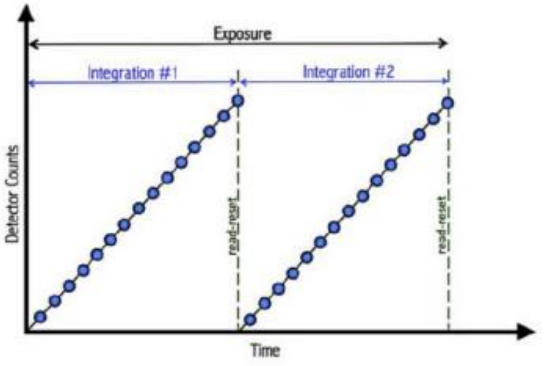

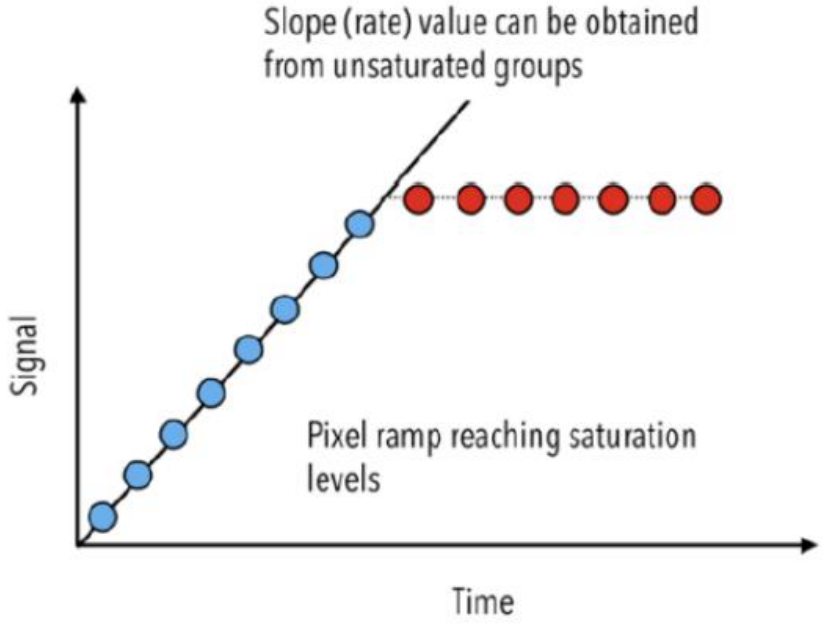

Images courtesy JWST Master Class 2020

Infrared Optics: Materials

Transmissive optical materials in the infrared are fewer and more expensive. Mostly reflective optical trains are needed to preserve long wavelengths.

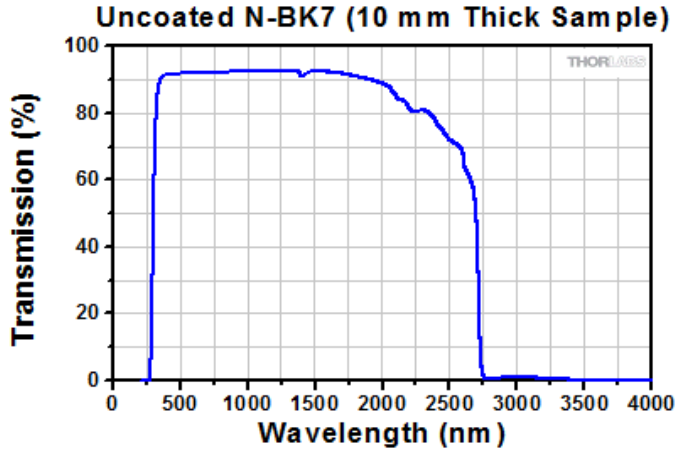

Properties of Optical Materials

Material	Abbe Number v_d	Coefficient of Thermal Expansion (10-6/°C)	Conductivity (W/m°C)	Heat Capacity (J/gm°C)	Density at 25°C (gm/cm3)	Knoop Hardness (kg/mm2)
BK 7	64.17	7.1	1.114	0.858	2.51	610
SF 2	33.85	8.4	0.735	0.498	3.86	410
UV Fused Silica	67.8	0.52	1.38	0.75	2.202	600
CaF_2	94.96	18.85	9.71	0.85	3.18	158
MgF_2	106.18	13.7 || to c axis 8.48 ⊥ to c axis	21 || to c axis 30 to ⊥ c axis	1.024	3.177	415
Crystal Quartz	69.87	7.1 to || c axis 13.2 ⊥ to c axis	10.4 || to c axis 6.2 ⊥ to c axis	0.74	2.649	740
Borofloat®	65.41	3.25	1.2	0.83	2.2	480
Zerodur®	56.09	0 ± 0.1	1.46	0.80	2.53	620
ZnSe	84.45	7.6	18.0	0.399	5.27	105

Common Optical Material Properties

Material	Transmission Range	Cost	Features
BK 7	380–2100 nm	Low	High transmission for visible to near infrared applications, the most common optical glass
UV Fused Silica (UVFS)	195–2100 nm	Moderate	Excellent homogeneity and low thermal expansion, high laser damage resistance
CaF_2	170–8000 nm	High	High transmission for deep UV to infrared applications
MgF_2	150–6500 nm	High	Birefringent material, excellent for use in the deep UV to infrared
ZnSe	600–16000 nm	High	Excellent choice for IR lens due to its broad wavelength range. Perfect candidate to use with high power infrared laser due to its low absorption coefficient.

Reference: Newport Tech Note: Optical Materials

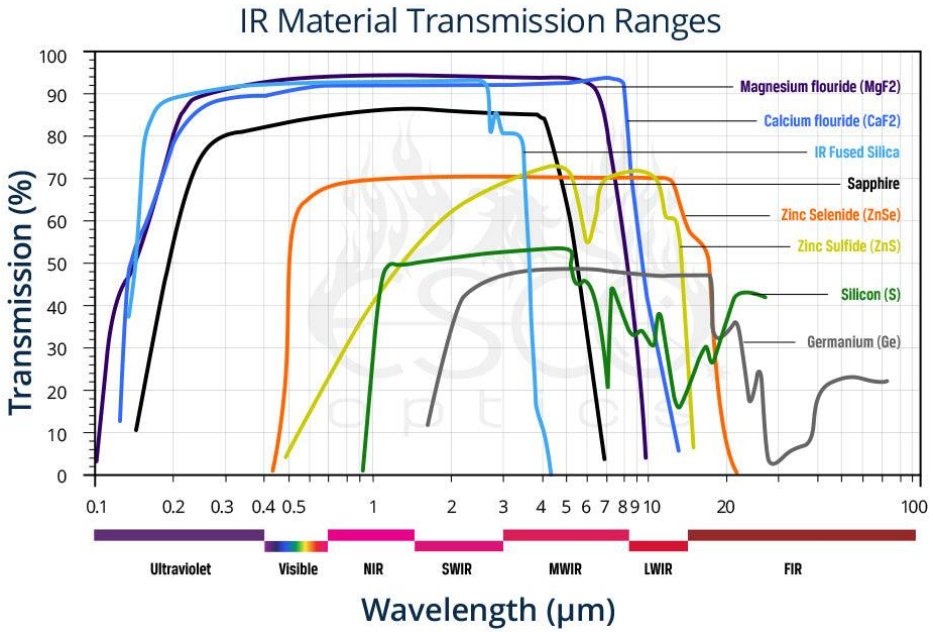

Reference: ESCO optics

Infrared Optics: Materials

Transmissive optical materials in the infrared are fewer and more expensive.
Mostly reflective optical trains are needed to preserve long wavelengths.

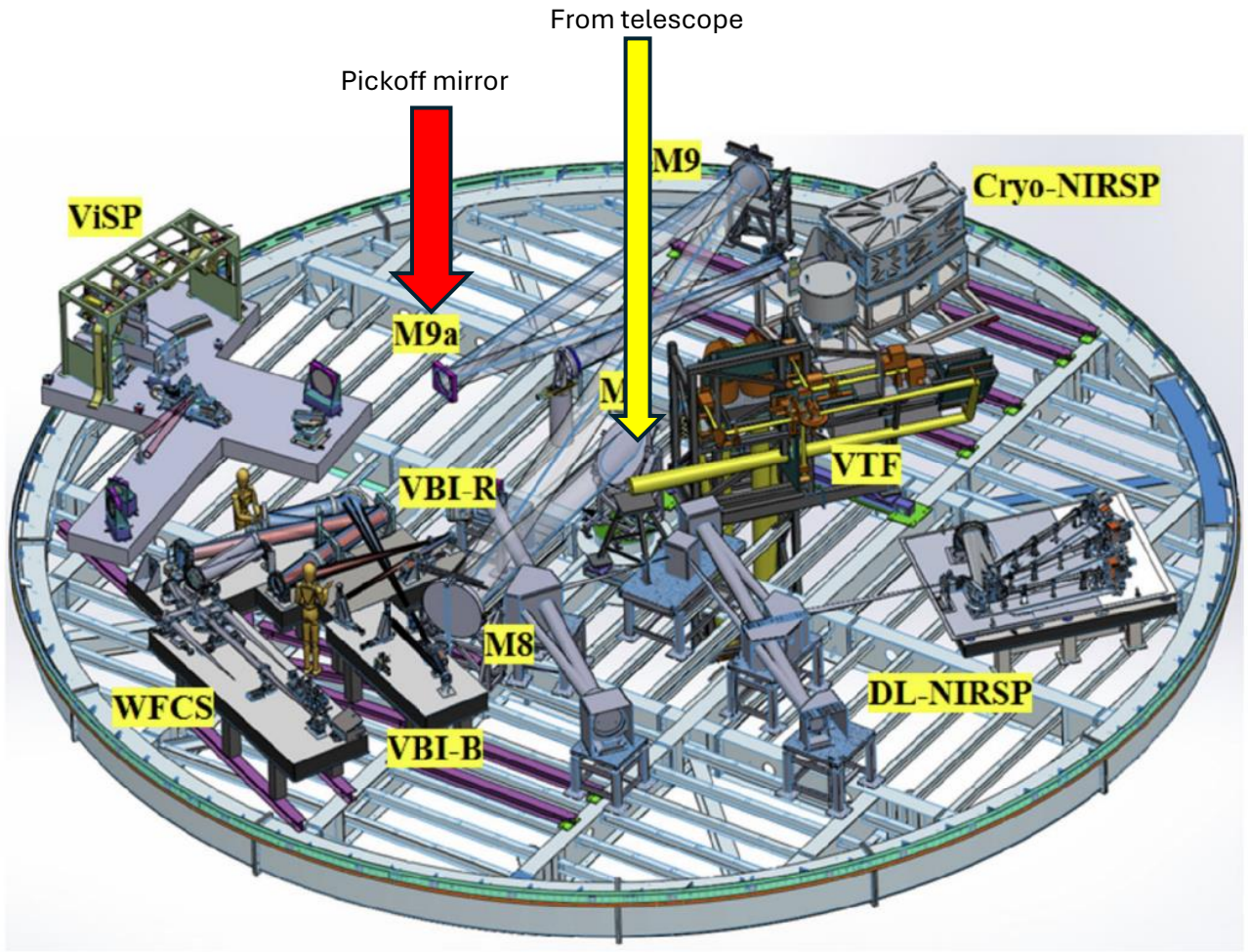

This is one of the fundamental reasons why DKIST/CryoNIRSP operates alone.

A fold mirror upstream of all transmissive optics in deployed into the beam when using CryoNIRSP.

Infrared Solar Telescopes: All-reflective designs

McMath-Pierce Solar Telescope
Kitt-Peak Arizona
(1962-2018)

Goode Solar Telescope
Big Bear, CA (2009-)

Daniel K Inouye Solar Telescope
Haleakala, Hawaii (2022-)

Other high-resolution ground-based facilities (esp. those built prior to ~2005) use an evacuated optical path to decrease internal thermal seeing effects, but at the cost of highly attenuated infrared transmission.

Swedish Solar Telescope: Entrance optical lens is ~80 mm thick fused silica.
Dunn Solar Telescope: Entrance/exit fused silica windows.

IR Instrumentation: Cooling requirements

Lower bandgap energies of IR cameras require cooling to maintain low dark and thermal background current.

IR cameras usually require deep cooling (~77 K). Thermal IR instruments also must cool upstream optics to reduce in-band thermal emission.

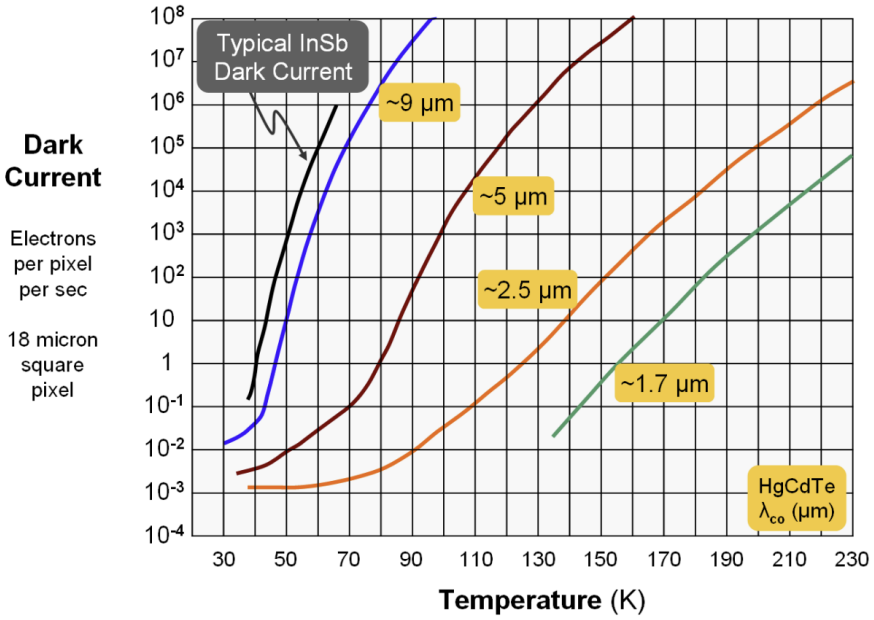

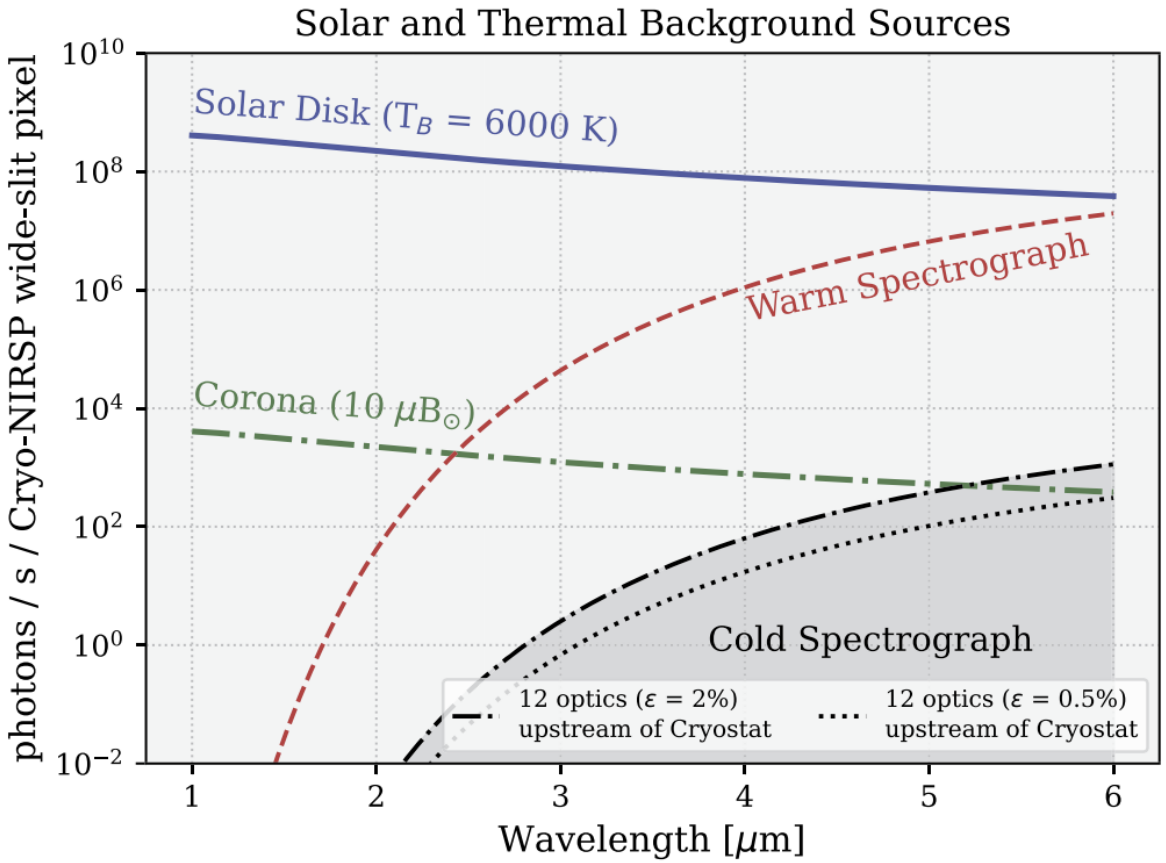

IR Instrumentation: The CryoNIRSP cryostat

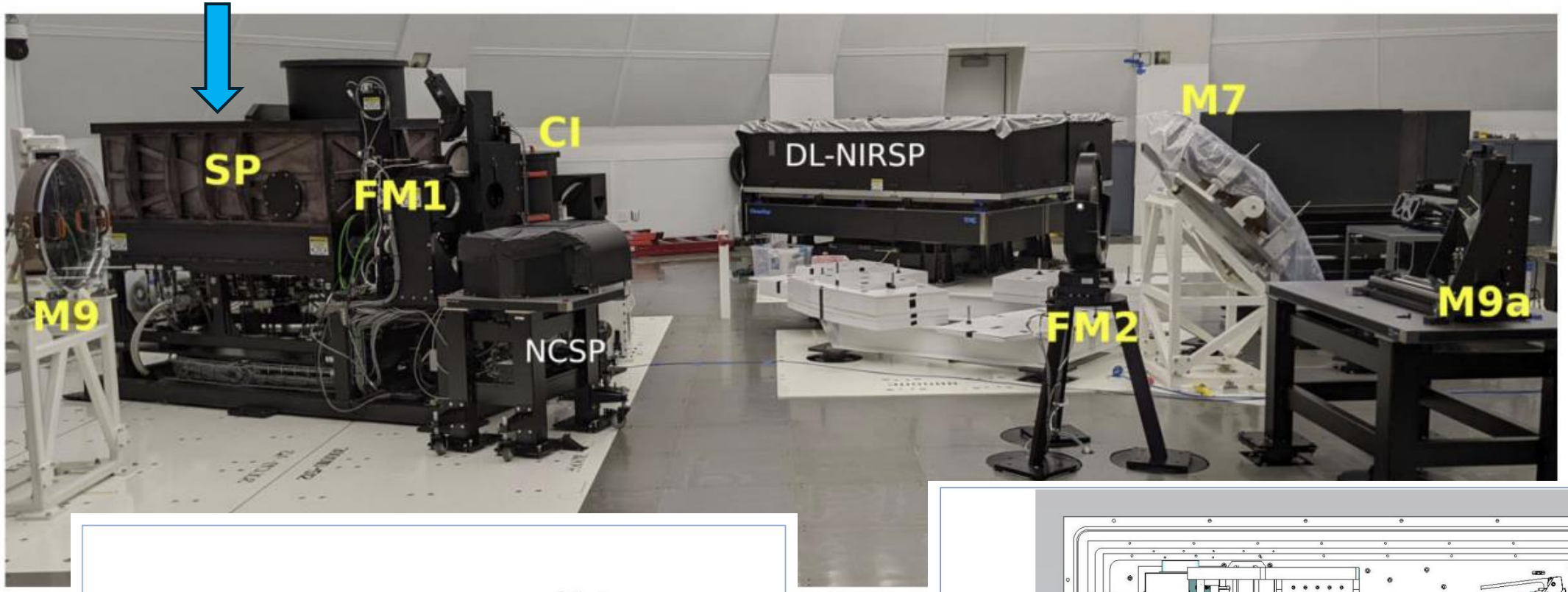

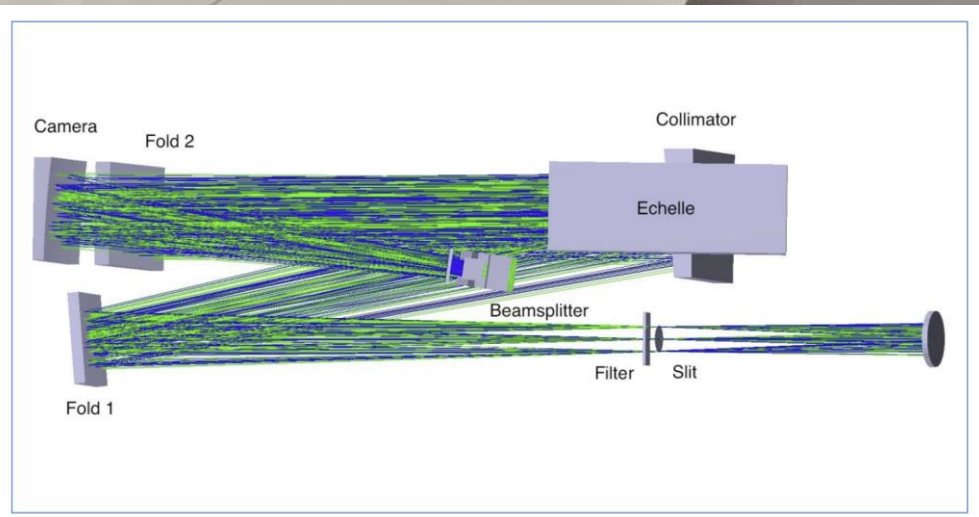

Figure 11: Spectrograph Zemax layout.

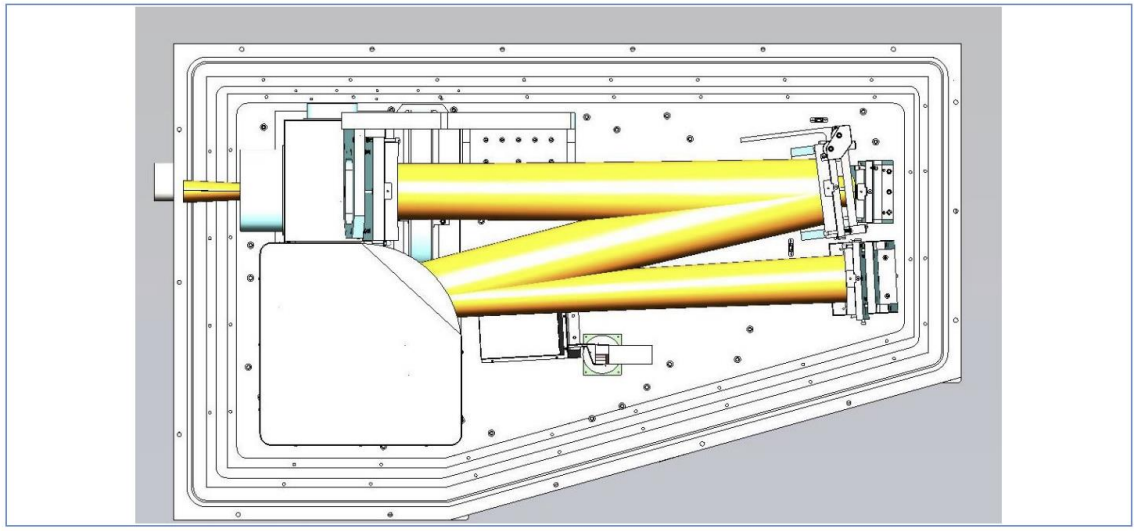

Figure 12: Spectrograph solid model with optics and mounts (top view).

The grating is located in a separate housing to reduce stray light.

IR Instrumentation: Coronagraphy

As previously mentioned, in the IR, scattered light properties of the sky and instrumentation are improved and the magnetic field sensitivity of emission lines enhanced.

This motivates the building of infrared performant coronagraphs.

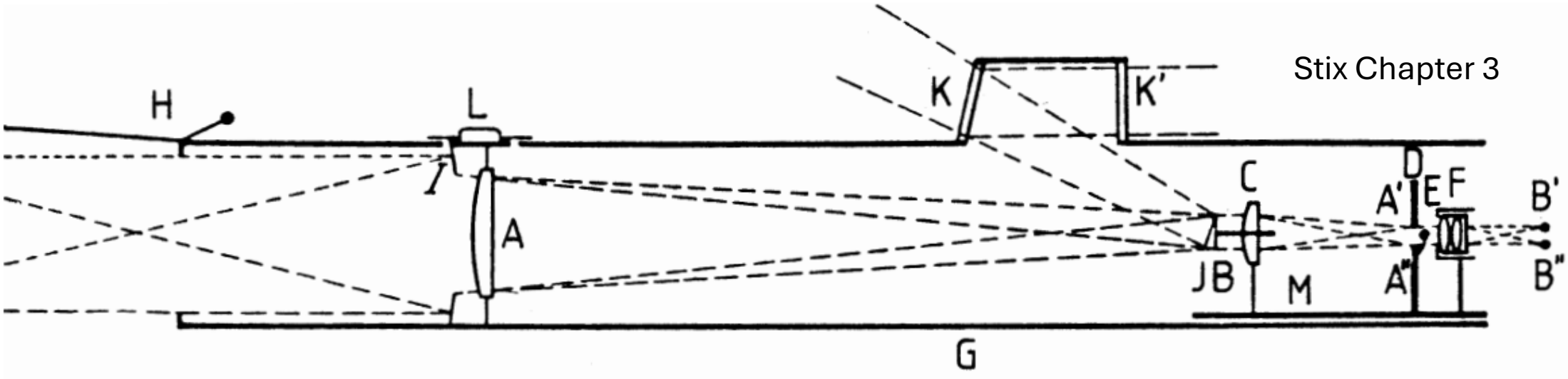

Fig. 3.46. Coronagraph. After Lyot (1932)

Classical Lyot coronagraph minimizes scatter at primary singlet objective and a pupil stop at D to below diffracted light at the edges of the objective.

IR Instrumentation: Coronagraphy

DKIST is an off-axis unobscured large-aperture coronagraph.

Inverse occulting at prime field stop, Lyot stop at pupil, secondary focus limb occulting.

In-situ cleaning helps maintain cleanliness of primary mirror.

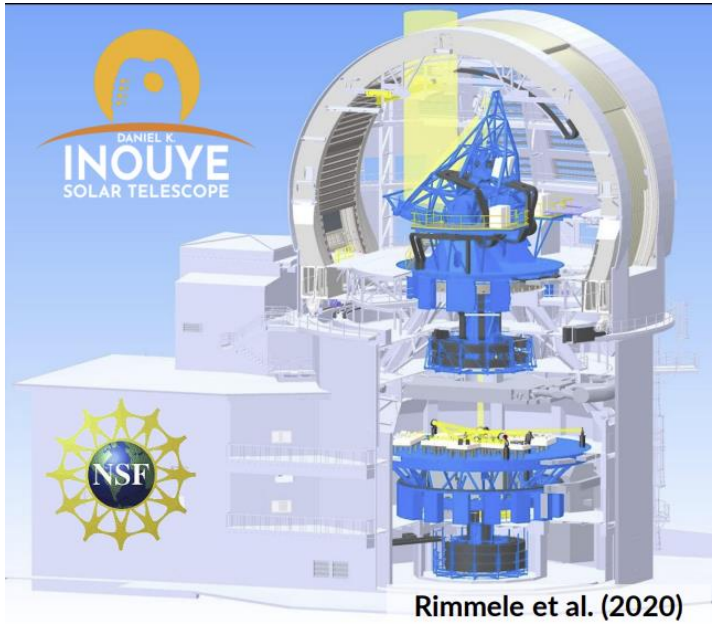

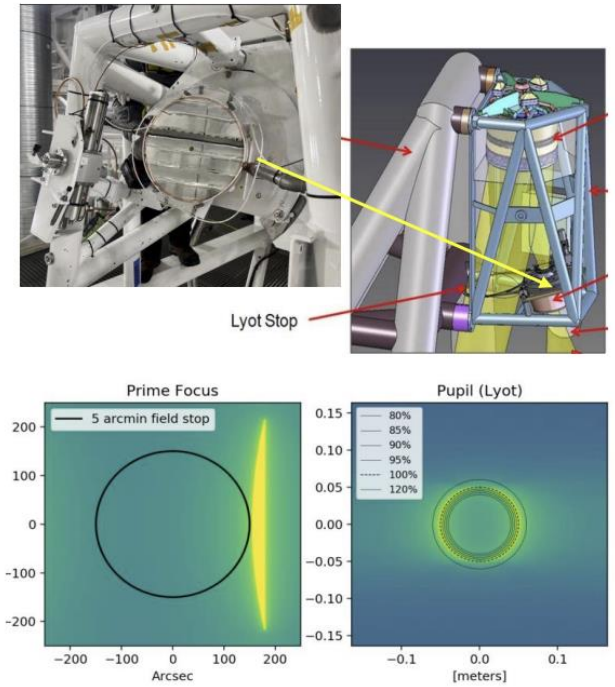

Lecture Outline - Summary

- Defining the Infrared: A short history
- The Infrared Solar Spectrum
  - Continuum formation and flare emission
  - Atomic lines of the lower atmosphere
  - Molecular species
  - Coronal emission
- Observing at Infrared Wavelengths
  - Advantages and disadvantages
  - Detectors
  - Optics
  - Cryostats
  - Coronagraphs
- **Summary and Outlook**
  - This afternoon's tutorial: Coronal IR Spectroscopy using DKIST/CryoNIRSP